

# Automatic recognition of maternal ECG in a fetal ECG lead

Master's thesis in Biomedical Engineering

MELANIE TORRES BISBAL

DEPARTMENT OF ELECTRICAL ENGINEERING

CHALMERS UNIVERSITY OF TECHNOLOGY

Gothenburg, Sweden 2021

[www.chalmers.se](http://www.chalmers.se)



MASTER'S THESIS 2021

# Automatic recognition of maternal ECG in a fetal ECG lead

Melanie Torres Bisbal



**CHALMERS**  
UNIVERSITY OF TECHNOLOGY

Department of Electrical Engineering  
*Division of Signal Processing and Biomedical Engineering*  
CHALMERS UNIVERSITY OF TECHNOLOGY  
Gothenburg, Sweden 2021

Automatic recognition of maternal ECG in a fetal ECG lead

© MELANIE TORRES BISBAL, 2021.

Supervisors: Mats Kjellstrand, Neoventa Medical and Anna Ragnerius, Neoventa Medical

Examiner: Sabine Reinfeldt, Department of Electrical Engineering

Master's Thesis 2021

Department of Electrical Engineering

Division of Signal Processing and Biomedical Engineering

Chalmers University of Technology

SE-412 96 Gothenburg

Telephone +46 31 772 1000

Cover: Original approach (top) and new approach (bottom) output from Neoventa STAN Viewer software.

Typeset in L<sup>A</sup>T<sub>E</sub>X

Gothenburg, Sweden 2021

Automatic recognition of maternal ECG in a fetal ECG lead  
MELANIE TORRES BISBAL  
Department of Electrical Engineering  
Chalmers University of Technology

## Abstract

This thesis was conducted in collaboration with the company Neoventa Medical. The company provides inventive fetal monitoring that aims for patient safety and supports clinicians in their decision making. In Neoventa's fetal surveillance monitors, the fetal ECG (FECG) function continuously calculates the fetal heart rate and several parameters of the FECG-waveform. The calculation is done based on the signal measured between the spiral electrode, attached to the fetal scalp, and two reference electrodes: the maternal thigh electrode and an electrode in the amniotic fluid. In rare cases, the maternal pulse can be seen in this signal. If this happens, there is a risk that the system measures the maternal pulse and presents it as if it was the fetal pulse.

Therefore, this thesis aims to modify the Neoventa solution in which the template of a heart beat is chosen to avoid that the maternal beat is not the base to calculate the heart rate and the FECG analysis. The solution differentiates between the maternal beats from the fetal beats and gives priority to the fetal ones.

A literature review was conducted to study the physiological differences between maternal and fetal beats. In addition, it was researched which methods are nowadays used regarding how to calculate fetal heart rate for both in fetal scalp approach and the usage of abdominal electrodes. Furthermore, statistics regarding the P-wave and the QRS width of fetal peaks were made and taken into account to develop an algorithm that gives priority to fetal beats over maternal ones.

Several preliminary studies were conducted with raw data files where the occurrences that maternal heart beats were presented as fetal beats. Based on these preliminary studies, a specific approach was chosen to improve the quality coverage of FECG. For reliable results and to ensure that the new approach has not decreased the quality, the approach was tested with a year of data provided by Neoventa which improved the coverage quality slightly (about 0.07%). However, the design can be further improved. For example by adapting the preprocessing of the data, which currently limits when a beat is acceptable but at the same time maintains a minimum quality of the template chosen. Another way in which the approach can be improved is by optimizing the weight of the different characteristics of the signal.

In conclusion, the development of this project was satisfactory since the new design has improved the FECG quality coverage.

Keywords: fetal, surveillance, ECG, heart, rate, maternal, STAN, FSE, FECG, FHR



# Acknowledgements

This thesis was written in collaboration with the company Neoventa Medical AB under the supervision of Mats Kjellstrand and Anna Ragnerius. I would like to thank my supervisors for supporting and helping me during the duration of this project. They were available when I needed advice in how to progress forward in both terms of study and environment, as well as for coding. In Neoventa medical, I would also like to express my gratitude to Annika Mårtendal who gave me an introduction about their product and state-of-the-art fetal surveillance, as well to Johan Sundberg for interviewing me and giving me the chance to write the thesis with them.

In addition, I would like to thank my examiner at Chalmers University of Technology, Sabine Reinfeldt. She gave me valuable feedback and guided me through the process of completing this thesis. Also, I want to thank one of my colleagues in the Biomedical Engineering master's, Sophie Stirl, who was a strong support reviewing the report.

I would like to express special thanks to my partner, Andreas Fransson, who has supported me through the entirety of my study period at Chalmers as well as throughout the development of this thesis from home. I want to thank my mom who always believes that I am capable of achieving my goals and supports me through them.

Furthermore, I want to thank my gaming buddies who have supported me while I was on the search for a thesis, when I found the topic and then encouraged me through the process of it. Thank you for making me able to enjoy my breaks from the thesis and keeping me sane.

And finally, I want to show appreciation for my two cute rats, Croqueta and Vermut, who kept me company and gave me cuddles during all the development of this thesis.

Melanie Torres Bisbal, Gothenburg, June 2021



# Contents

<b>List of Figures</b>	<b>xi</b>
<b>List of Tables</b>	<b>xiii</b>
<b>1 Introduction</b>	<b>1</b>
1.1 Background . . . . .	1
1.2 Aim . . . . .	4
1.3 Specification of issue under investigation . . . . .	4
1.4 Limitations . . . . .	5
1.5 Ethical considerations . . . . .	6
<b>2 Theory</b>	<b>7</b>
2.1 The heart . . . . .	7
2.2 The ECG complex . . . . .	8
2.3 Fetal surveillance and Neoventa . . . . .	9
2.4 Diverse ECG configurations . . . . .	11
2.5 Literature review . . . . .	12
<b>3 Methods</b>	<b>15</b>
3.1 Tools . . . . .	15
3.2 Data . . . . .	19
3.3 Design of the algorithm . . . . .	21
3.3.1 Common sections . . . . .	21
3.3.2 First approach regarding the width of the QRS complex . . . . .	25
3.3.3 Second approach regarding the width of the QRS complex . . . . .	27
<b>4 Results</b>	<b>33</b>
4.1 Preliminary results . . . . .	33
4.1.1 Data used . . . . .	33
4.1.2 First approach regarding the width of the QRS complex . . . . .	34
4.1.3 Second approach regarding the width of the QRS complex . . . . .	39
4.2 Final results with Neoventa database . . . . .	43
<b>5 Discussion</b>	<b>45</b>
5.1 Common parts . . . . .	45
5.2 First approach regarding the width of the QRS complex . . . . .	47
5.3 Second approach regarding the width of the QRS complex . . . . .	48

## Contents

---

5.4	Neoventa database . . . . .	53
5.5	Future work . . . . .	53
<b>6</b>	<b>Conclusion</b>	<b>55</b>
	<b>Bibliography</b>	<b>57</b>
<b>A</b>	<b>Appendix 1</b>	<b>I</b>

# List of Figures

1.1	ECG signal [3] . . . . .	2
1.2	Diagram of the FHR algorithm . . . . .	3
1.3	FECG signal processing on block level . . . . .	4
2.1	Human heart displaying the sections, image from [8] . . . . .	8
2.2	Heart contraction correlated with ECG [10] . . . . .	9
2.3	FSE . . . . .	10
2.4	FECG leads in STAN with different configurations in spiral – skin lead	11
3.1	Raw Data Viewer . . . . .	15
3.2	Stan Viewer 2 . . . . .	16
3.3	Stan Viewer 3 . . . . .	16
3.4	STN diagnostics tool . . . . .	17
3.5	STN diagnostics output . . . . .	17
3.6	Histogram of the mean value of the P-wave (round 3 decimals) . . . . .	18
3.7	Recording Details tool . . . . .	19
3.8	Score position used . . . . .	22
3.9	Histogram of the QRS amplitude with one year data of the database	23
3.10	Histogram of the output of Equation 3.3 . . . . .	24
3.11	Loop left side of the R-peak . . . . .	26
3.12	Loop right side of the R-peak . . . . .	26
3.13	Loop left side of the S-peak . . . . .	27
3.14	Loop right side of the S-peak . . . . .	27
3.15	Width in the 50% duration . . . . .	28
3.16	Histogram of the width in the 50% part of the peak . . . . .	29
3.17	Looping left to find the position in the 50% duration . . . . .	29
3.18	Looping right to find the position in the 50% duration . . . . .	29
3.19	Example maternal beat 50% width . . . . .	30
3.20	Example maternal beat 50% width . . . . .	30
3.21	Example maternal beat 50% width . . . . .	31
3.22	Example maternal beat 50% width . . . . .	31
3.23	Example fetal beat 50% width . . . . .	31
4.1	0281 output of the first approach with rejection . . . . .	35
4.2	1331 output of the first approach with rejection . . . . .	35
4.3	1374 output of the first approach with rejection . . . . .	36
4.4	1294 output of the first approach with rejection . . . . .	36

4.5	0281 output of the first approach with no rejection . . . . .	37
4.6	1331 output of the first approach with no rejection . . . . .	38
4.7	1374 output of the first approach with no rejection . . . . .	38
4.8	1294 output of the first approach with no rejection . . . . .	38
4.9	0281 output of the second approach with rejection . . . . .	39
4.10	1331 output of the second approach with rejection . . . . .	40
4.11	1374 output of the second approach with rejection . . . . .	40
4.12	1294 output of the second approach with rejection . . . . .	40
4.13	0281 output of the second approach with no rejection . . . . .	41
4.14	1331 output of the second approach with no rejection . . . . .	42
4.15	1374 output of the second approach with no rejection . . . . .	42
4.16	1294 output of the second approach with no rejection . . . . .	42
5.1	Wrong peak is chosen with low score amplitude . . . . .	46
5.2	Good peak is chosen with low score amplitude . . . . .	47
5.3	Good result example with peaks and measurements . . . . .	48
5.4	Good result example with peaks and measurements . . . . .	49
5.5	Good result example with peaks and measurements . . . . .	49
5.6	Good result example with peaks and measurements . . . . .	50
5.7	Bad result example with peaks and measurements . . . . .	51
5.8	Good result example with peaks and measurements . . . . .	51
5.9	Good result example with peaks and measurements . . . . .	52
5.10	Good result example with peaks and measurements . . . . .	52
A.1	Histogram of the mean value of the P-wave (round 2 decimals) . . . . .	I
A.2	Histogram of the number of P-waves . . . . .	II
A.3	Histogram of minimum P-wave value . . . . .	II
A.4	Histogram of maximum P-wave value . . . . .	III
A.5	Histogram of median P-wave value . . . . .	III
A.6	Histogram of the 20% percentile of the P-wave value . . . . .	IV
A.7	Histogram of the 40% percentile of the P-wave value . . . . .	IV
A.8	Histogram of the 60% percentile of the P-wave value . . . . .	V
A.9	Histogram of the 80% percentile of the P-wave value . . . . .	V
A.10	Histogram of the 90% percentile of the P-wave value . . . . .	VI
A.11	Histogram of the 95% percentile of the P-wave value . . . . .	VI
A.12	Histogram of the 97% percentile of the P-wave value . . . . .	VII

# List of Tables

2.1	QRS duration (ms) as Average (and Upper limit of Normal) [25] . . .	13
3.1	Amount of files used and hours of recording from the Neoventa database	20
4.1	Original algorithm results . . . . .	34
4.2	First approach with rejection algorithm results . . . . .	35
4.3	First approach with no rejection algorithm results . . . . .	37
4.4	Second approach with rejection algorithm results . . . . .	39
4.5	Second approach with no rejection algorithm results . . . . .	41
4.6	Difference between new and old design results with Neoventa database	43
5.1	Scores of Figure 5.1 part 1 . . . . .	46
5.2	Scores of Figure 5.1 part 2 . . . . .	46
5.3	Scores of Figure 5.2 . . . . .	47
5.4	Scores of Figure 5.3 . . . . .	48
5.5	Scores of Figure 5.4 . . . . .	49
5.6	Scores of Figure 5.5 . . . . .	50
5.7	Scores of Figure 5.6 . . . . .	50
5.8	Scores of Figure 5.7 . . . . .	51
5.9	Scores of Figure 5.8 . . . . .	51
5.10	Scores of Figure 5.9 . . . . .	52
5.11	Scores of Figure 5.10 . . . . .	53



# 1

## Introduction

This chapter introduces the relevant topics for a profound understanding of the thesis work. The chapter contains background, aim, specifications under issue, limitations of the project and ethical considerations.

### 1.1 Background

Being born is the biggest challenge in the life of a person. To be able to endure labour, the fetus has several defense mechanisms against oxygen deficiency but the resources do not last forever [1]. For that reason, surveillance during labour is an excellent tool to assess the stress of the fetus. Furthermore, adequate support can be given to the clinicians who can then decide if a surgical intervention is needed to avoid oxygen deficiency leading to long-term damage such as cerebral palsy.

Neovanta Medical AB, hereinafter referred to as Neovanta, is a medical device company with headquarters in Gothenburg, Sweden founded by Professor KG Rosén [2]. Neovanta's solution provides inventive fetal monitoring that aims for patient safety and supports clinicians in their decision making. The main advantage and skill of Neovanta is in using the STAN fetal monitor to apply ST-analysis of the fetal Electrocardiogram (ECG) combined with Cardiotocography (CTG) during labour. In Figure 1.1, an ECG signal can be seen as well as the relevant part that concerns the ST-segment which corresponds to the ability of the fetal heart muscle to respond [1]. The main goal with STAN fetal monitoring is to measure the ST-segment and make an analysis based on it. To make the ST-analysis possible, Neovanta uses a Fetal Scalp Electrode (FSE) for internal monitoring instead of using ultrasound to calculate the Fetal Heart Rate (FHR) since it can not be achieved in any other way.

In Neovanta's fetal surveillance monitors there is a Fetal ECG (FECG) function that continuously calculates the FHR, as well as certain parameters of the FECG [4]. The calculation is done based on a signal measured between the spiral electrode, attached to the fetal scalp, and two reference electrodes: the maternal thigh electrode and an electrode in the amniotic fluid.

From the statistical data provided by Neovanta, it is known that there is often some weak maternal influence in the ECG signal where the impact of the amplitude of the maternal beats ranges between 'unrecognizable' and  $50\mu V$ .

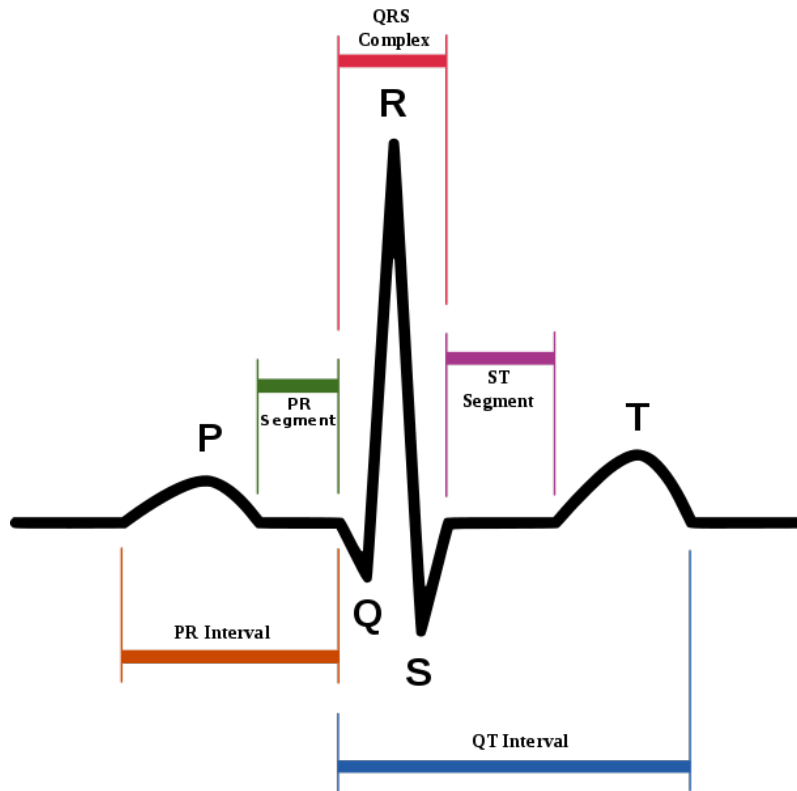


**Figure 1.1:** ECG signal [3]

However, the fetal beats are between  $50\mu\text{V}$  and  $750\mu\text{V}$ . In rare cases the ranges overlap, for example when the maternal beat is in the maximum of the statistical range,  $50\mu\text{V}$ , and the fetal beat is at the minimum of its range, also  $50\mu\text{V}$ . Other situations can be that the FSE is attached to the cervix, or in case of a dead fetus. When the maternal heart beat is recorded, in the signal there is a risk that the system measures the maternal pulse and presents it as the fetal pulse. This will impact the calculations of the ST-analysis and will therefore provide wrong information to the clinicians. This may affect their decision making which could delay a needed intervention or cause an unnecessary surgery.

The main steps of the FHR detection algorithm can be seen in Figure 1.2. First of all, an FHR template is established. Next, the template is used to detect fetal heart beats by continuously comparing it to the signal. The best match within a time period from the previous beat is considered the next beat, and the interval between them is used to calculate a Heart Rate (HR) value. If there is no good enough match for a certain time period, the FHR template is abandoned, and the device stops displaying an FHR value. Then the algorithm returns to find a new FHR template. Since the appearance of the QRS complex changes during labour, the algorithm constantly improves the FHR template. Also, since the quality of the signal in the spiral-to-scalp reference lead is sometimes poor, an FHR template is also established in the spiral-to-skin lead. In addition, FHR detection is provided as well during temporary loss of signal in the spiral-to-scalp.ref lead.

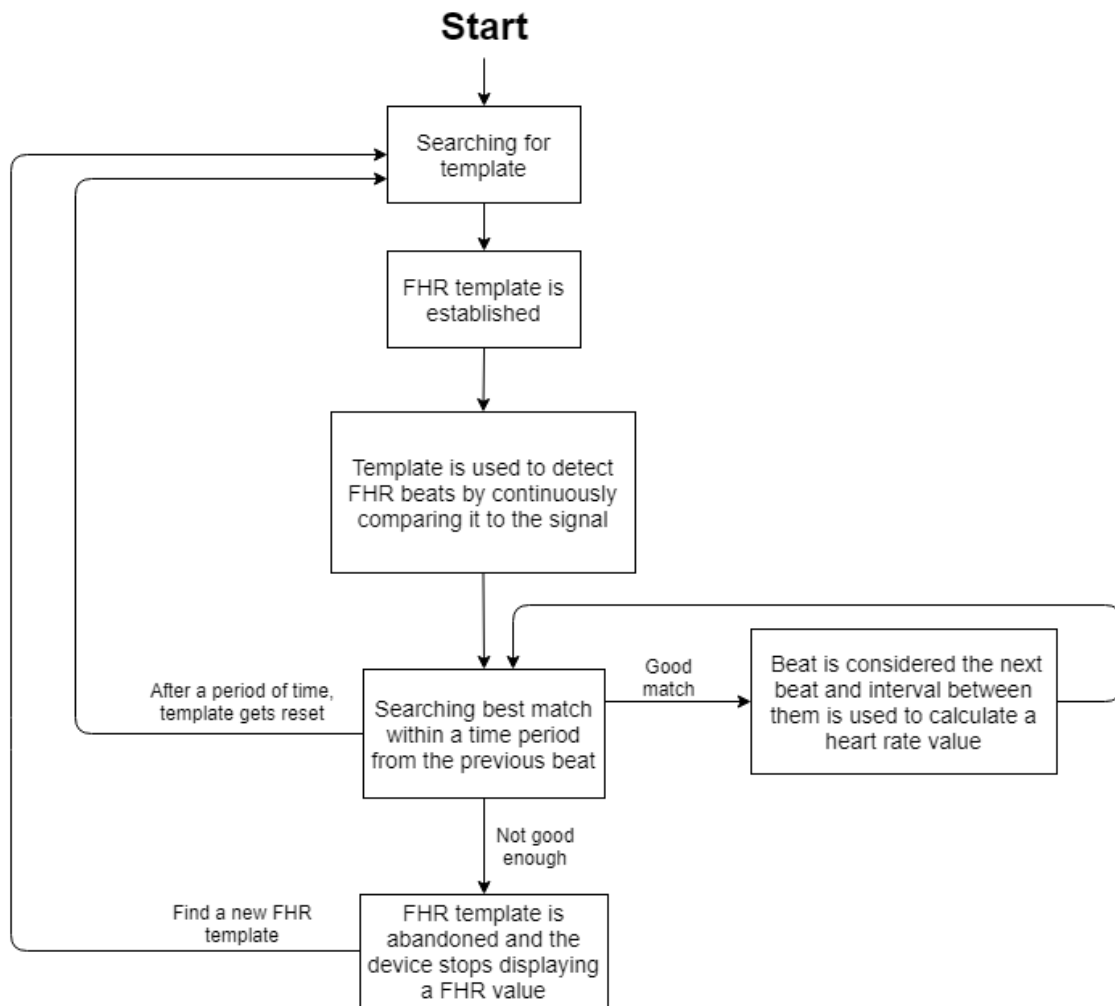


**Figure 1.2:** Diagram of the FHR algorithm

The FECG signal processing on block level can be seen in Figure 1.3. The next step, after the FHR is detected, is to perform the ST-analysis. The algorithm for analyzing the ST part averages 30 beats. For a beat to be added to the average, the signal has to fulfil certain criteria which will not be explained in detail here.

When the number of approved complexes reaches 30, the T/QRS ratio and some quality measures are calculated. Also, some additional rejection mechanisms are applied depending on the content of the average's waveform, which cannot be made on individual complexes. Then a trend analysis is conducted on the T/QRS ratios and when certain criteria are fulfilled, an ST-event will be launched and it is up to the clinician to act in relation to it.

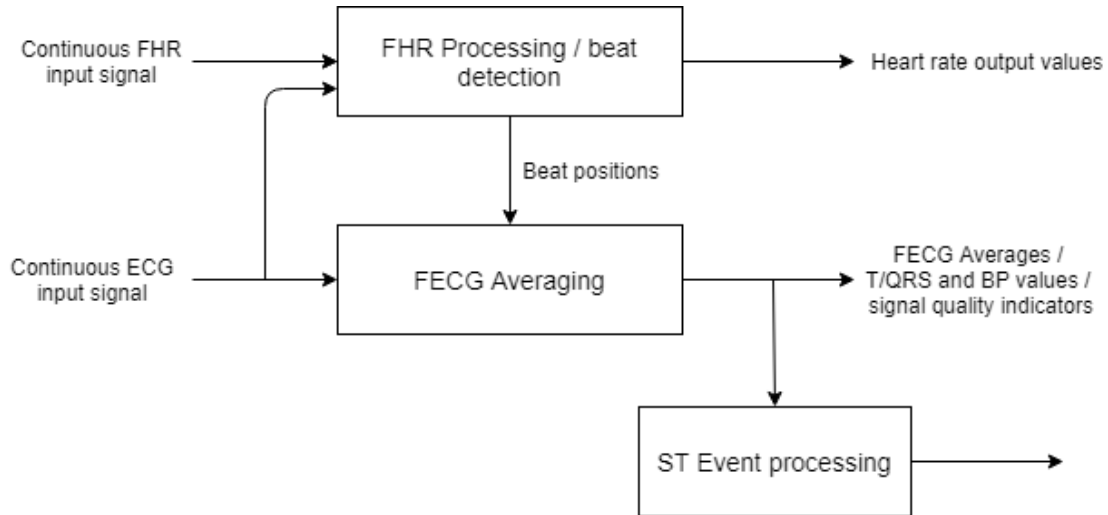


**Figure 1.3:** FECG signal processing on block level

## 1.2 Aim

The goal of the project is to modify the part in which a beat is acceptable to consider as a template. It can be both implemented at the beginning, when the first FHR template is decided, as well as when it gets updated when the QRS complex changes over time. In detail, the aim is to implement an algorithm that identifies situations when the maternal heart beat becomes the base for calculations of the FHR and FECG analysis and instead gives priority to the fetal beats.

In addition to the above, different actions could be taken. This includes to momentarily inhibit the FHR calculations, to momentarily inhibit the waveform analysis, to activate a warning message to the user of the system or to give priority to the fetal beats.

## 1.3 Specification of issue under investigation

There are several risk scenarios where the FHR is not correctly calculated. These are handled during the duration of the project:

- The algorithms for FHR detection may pick up a Maternal Heart Rate (MHR) from the very beginning of a recording when the first FHR detection template is selected, and start to present the MHR instead of FHR.
- The algorithms for FHR detection may switch to a MHR when the FHR detection template (spiral-to-scalp reference lead) is evolved with statistical data from the previous minute's processing.
- When the algorithms for FHR detection selects the secondary template for detecting beats in the spiral-to-skin lead, it may accidentally pick a maternal-like template and start to present the MHR instead of the FHR.
- Strong artifacts from other equipment may cause beat-like artifacts, then picked as FHR templates and then presented as a false FHR trace.

To mitigate the risks, there are several potential approaches that could be taken such as:

- Reject the proposed FHR detection template if it appears to have a shape of an adult HR.
- Reject FECG average waveforms if they appear to have a shape of an adult HR and show a technical alarm.
- Show a technical alarm or a warning message.
- Implement a more heuristic template selection mechanism. For example, measure the P wave and the width of the QRS complex.

From the expertise of the Neoventa team, it is known that the incidence of picking the MHR from the beginning is rare and there is no available data of it when using the FSE. This is due that the signal is much stronger for the fetal beat than the maternal beat with this kind of electrode. There are several recordings where the detection switches to maternal beats, but it is unknown what happened in the transition. Furthermore, it is rare to record strong artifacts from external machines which are often perceived by the midwife as an artificial trace and therefore discarded.

There are several considerations that can be taken into account when finding the most optimal mitigation. Some examples are:

- The customer needs a high availability of FHR data, especially customers that are running ST-analysis where the availability of FHR data affects the availability of the ST-analysis.
- Automatic measures are preferred compared to measures where the user needs to make adjustments or interpret technical alarm messages.
- Not all hospital technicians have access to FECG simulators who expect to be able to conduct function tests using an adult ECG simulator.

## 1.4 Limitations

Within this project, the calculation for the ST-analysis is not modified; the main goal is to rework what is acceptable to use as the base for FHR. Apart from that, the programming environment can be a technical limitation on this project which is developed in Visual Studio 2010 using C++05. This could mean that some available frameworks are not compatible with it. However, it is not the goal of this project to update the existing code to more recent versions.

## 1.5 Ethical considerations

Most of the data that is used in this project represent real life recordings from patients. The traces must be presented so that they can not be linked back to the patient. Hospitals generally remove personal identification such as patient name, ID and annotations recorded by the midwife when they send recording files to Neoventa, and Neoventa always make sure there is no remaining personal information in any recording files it receives.

The outcome of this project is important for society since by improving the tools that are already available for fetal surveillance, the number of cesarean section can be decreased [5]. Furthermore, the number of babies born with oxygen deficiency may be reduced [1].

# 2

## Theory

This chapter covers an overview of the main concepts to understand where an ECG comes from and how the heart works. In addition, the chapter includes a background about fetal surveillance and the work that Neoventa does as well as the outcomes of the literature study.

### 2.1 The heart

The heart is an organ made out of muscle tissue which functions as a pump that receives blood and distributes it to different sections of the body [6]. The organ is located in the space between the lungs in the center of the chest. The heart of an adult is 12 cm long, 9 cm wide and 6 cm thick. It weighs around 250 and 350 grams. An approximation of the size of the heart can be done by checking the size of a person's fist. In comparison, a normal fetal heart size is about one third of the thorax, also the heart's diagonal diameter should not be bigger than half of the chest's diagonal diameter [7].

An image of the heart can be seen in Figure 2.1. The heart consists of four chambers namely the two upper chambers which are called the atria and the two lower chambers which are referred to as ventricles [6]. The goal of the atria is to collect blood. The right atrium takes low oxygenated blood from the superior vena cava and the coronary sinus. The left atrium gets oxygenated blood from the lungs by the pulmonary veins. The purpose of the ventricles is to pump blood. While the right ventricle provides blood to the lungs, the left ventricle sends the blood to the body. In addition, atrioventricular valves divide the atria and ventricles from each other.

The cardiac cycle can be defined as the process in which all the events related to a heartbeat occur [6, 9]. First, the atria contract and the ventricles relax. Next, when the ventricles contract the atria relax. These phases are called systole and diastole respectively. In systole, when the chambers are contracted, the blood is ejected while in the diastole, the heart relaxes and the chambers fill with blood. In addition, the Cardiac Output (CO) describes how much blood is pumped by the heart to the aorta every minute.

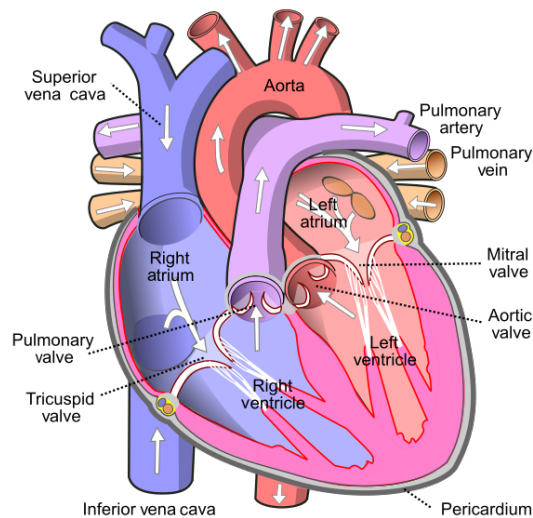


**Figure 2.1:** Human heart displaying the sections, image from [8]

The pacemaker cells are a unique characteristic of the heart compared to cells in other organs because they can create electrical impulses without having to be excited by nerves [6]. Also, there is another type of cardiac cell which have an mechanical function called contractile cells. For example, myocardial cells contain filaments that contract when the cell receives an electrical stimulation.

## 2.2 The ECG complex

To understand how an ECG is formed, it is needed to understand how charged particles work. One type of particles are electrons which are negative charged as a result of a chemical reaction [6, 9]. Another important concept to know is that the flow of electrical charge from a specific position to another is the current. Voltage is defined as the measurement between two points which have separated electrical charges of an opposite polarity.

The electrical current that can be measured in the human body has origin in the body fluids that contains electrolytes which have charged particles [6]. As a result of this, fluids in the body that have this specific composition can conduct current through it. The difference in concentration across the cell membranes makes them being able to get excited.

Furthermore, the membrane potential is defined as the voltage across the cell membrane [6]. For example, what it is shown in an ECG as spikes or waveforms is the variations of the voltage. When the inside is more negative than the exterior, the cell is in a polarized state. When this cell is stimulated the membrane changes and it can absorb  $\text{Na}^+$  and  $\text{K}^+$ . This change of state makes it able to allow to pass electrolytes. Next,  $\text{Na}^+$  can enter the cell which causes the cell to become more positively charged inside than on the outside. This electricity variation can

be recorded on the ECG as spikes. Then, the charged particles in between the cell membranes move across which makes the inside of the cell more positively charged. This process is defined as depolarization.

An image showing the different contractions of the heart and correlated with each part of the ECG can be seen in Figure 2.2. In the specific case of the heart, a P-wave can be observed in the ECG when the atria are stimulated which is named atrial depolarization. Furthermore, a QRS complex can be observed in the ECG when the ventricles are stimulated which is referred to as the ventricular depolarization. Afterwards, the cell recovers and returns to its normal electrical potential. The ST segment and T-wave in the ECG appear when the ventricular repolarization happens.

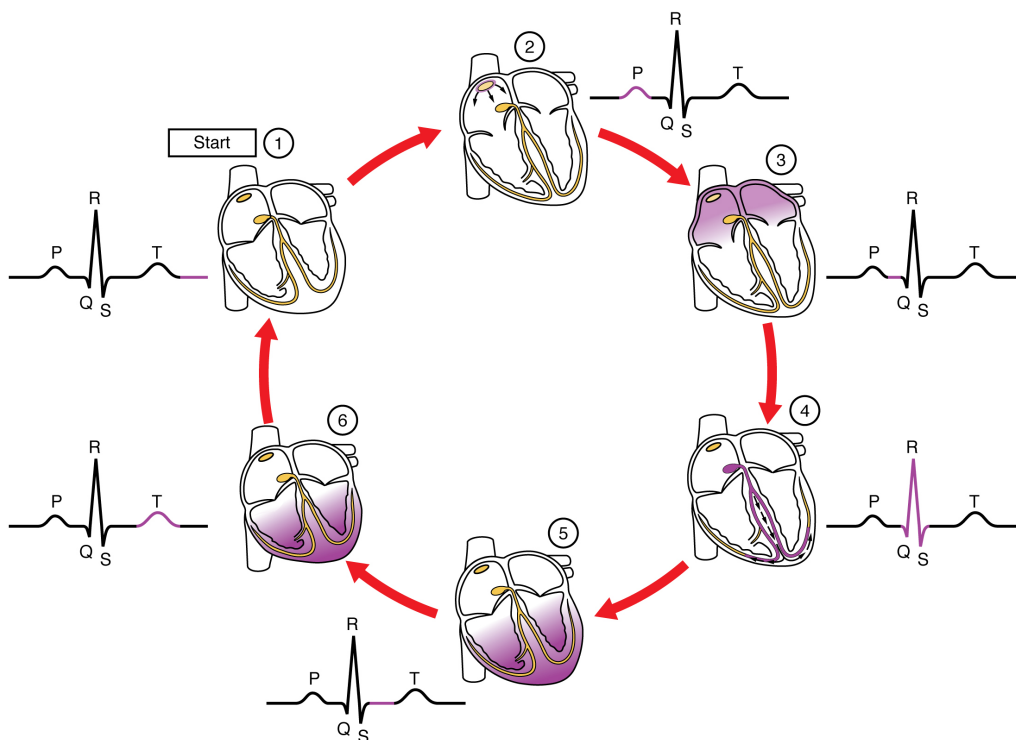


**Figure 2.2:** Heart contraction correlated with ECG [10]

### 2.3 Fetal surveillance and Neoventa

Fetal surveillance is a broad term which consists of the monitoring of the fetus. For example, it can be applied during childbirth to ensure a safe delivery [11]. In developed countries, the most common tool to use during labour is Cardiotocography (CTG) even though there is little evidence of its success regarding to reduce long-term neurological deaths and metabolic acidosis [12]. The results of long-term studies indicate that CTG often leads to unnecessary interventions; one of them is the increase of cesarean sections within the last years [12, 13].

In addition, ST-analysis of the FECG, in other words the STAN® method, was introduced around 2000 after several years of researching about the physiology of fetal surveillance which is applicable and useful during childbirth [12]. For example, one of the outcome of the animal studies and the reason why the STAN® method is interesting to be applied during delivery is that researchers found a correlation between the ST-segment in the FECG and fetal hypoxia. Neoventa developed electronics and algorithms with sufficient sensitivity to monitor the ST-segment, also conducted studies to prove its clinical usefulness. To be clinically useful, the clinician has to consider the long-term ST-waveform changes together with the CTG (i.e. FHR changes and uterine contractions).

Neoventa's mission is to assist professionals and improve obstetrician care worldwide [14]. The way in which Neoventa differentiates from other competitors is by improving the state-of-the-art by offering their solution based on ST-analysis of the FECG, which is the only method that has evidence to reduce neurological damage and operative deliveries while also being cost-effective [15, 16]. Neoventa also has other products such as disposable FSEs for the use of internal monitoring branded under the Goldtrace name which can be seen in Figure 2.3a and Figure 2.3b.

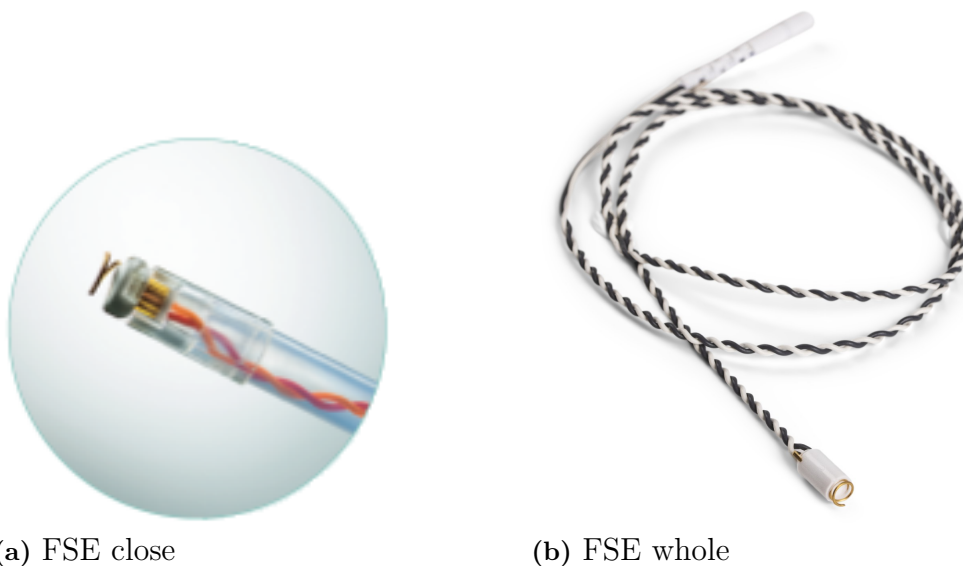


**Figure 2.3:** FSE

A possible configuration in which the STAN® method can be used with FSE are the following FECG leads. The leads are based on three leadwires: one spiral rotated into the scalp, a reference electrode in amniotic fluid and a reference skin electrode on maternal thigh. A close image of the FSE can be seen in Figure 2.3a and the whole FSE can be seen in Figure 2.3b. As a result of different combination of the leadwires there are three FECG leads; spiral to scalp reference which is used for FHR detection only, spiral to skin which is used for ST-analysis and supporting the FHR detection and scalp reference to skin which is unused today.

The technique used in the STAN<sup>®</sup> method is based on the concept to use the fact that the changes of the ST-interval are related to the fetal myocardium when there is a lack of oxygen [17]. The changes in the FECG that are significant for fetal distress can be an increase in the T-wave amplitude having a base measurement formed on QRS amplitude, in other words having a T/QRS ratio. The STAN<sup>®</sup> guidelines and the use of ST-analysis is indicated for 36 weeks and later [12].

## 2.4 Diverse ECG configurations

In section 2.2, the origin of the ECG complex was explained as well as which processes of the heart correlate with each part of the ECG complex waves. Unfortunately, not all ECGs look the same and it can be challenging to measure specific parts of the ECG complex, for example the QRS duration.

This also applies to the FECG leads in STAN<sup>®</sup> and can vary with different configurations in spiral - skin lead. Several FECG results using a variety of configurations can be seen in Figure 2.4. To understand the differences and how to refer to the complexes, different notations are made: small deflections are reflected using lower case, and larger deflections with upper case. A first downwards deflection is a Q (or q) and negative deflection is notated as an S. On the other hand, an upward deflection is an R, if it is the same deflection it is stated with a prime, for example as R'.

Based on 4831 recordings from the Neoventa database, it can be stated that in normal recordings the most common complexes are qRs. However, qR are also occurring frequently. Furthermore, split-R (R') appear in 7% of the recordings.

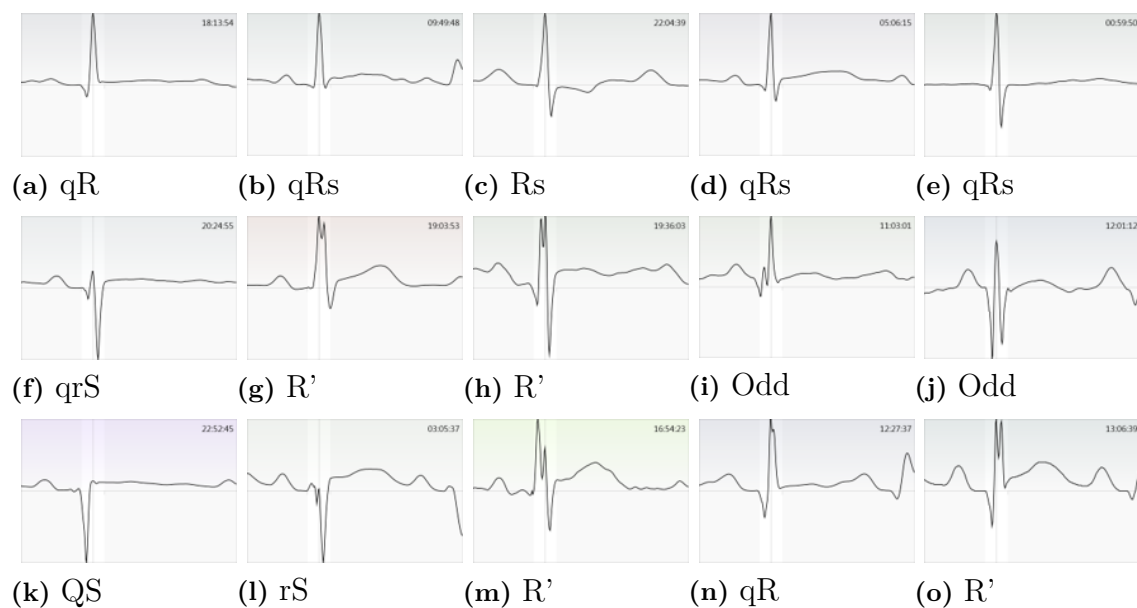


**Figure 2.4:** FECG leads in STAN with different configurations in spiral – skin lead

## 2.5 Literature review

At the beginning of the project, it was critical to perform a literature study to find evidence in how the Maternal ECG (MECG) differs from the FECG. Another search was conducted to see how the noise is eliminated to obtain the FECG in different setups such as abdominal ECG or when using an FSE. For this purpose, PubMed, Google scholar, Chalmers library and other search engines focused on research were utilized. In addition, Zotero was used to manage papers, books and references.

The first investigation focused on how MECG noise is reduced in the current state of the art. Some of the different methods that are used for reducing the maternal influence are adaptive filtering methods, linear decomposition methods, nonlinear decomposition methods and wavelet decomposition [18]. Adaptive filtering methods train a matched filter to remove the MECG, the downside of those is that they need a specific reference maternal lead. On the other hand, linear methods divide the signal into different parts as MECG, FECG and noise. These methods can include Kalman Filtering, Volterra Filtering, Comb Filtering, Least Mean Squares among others [19]. In addition, artificial intelligence can be used and it is the case in which nonlinear methods are implemented. These can include adaptive neural networks, hybrid neural networks and other configurations. Another applicable method is the wavelet decomposition which transforms the signal to the wavelet domain to denoise it and separate in different components. Most of the information found was about non-invasive FECG and using an FSE as a reference.

One of the outcomes of the literature review was the duration of the different time intervals for FECG and MECG. The most common duration of the QRS complex in the FECG is from 20 ms to 50 ms and the duration above 60 ms is uncommon [20]. There has been a systematic review of cardiac time intervals depending on the term of the pregnancy [21]. For this project, the important values are when the pregnancy is at least 36 weeks since the STAN guidelines can be applied and the tool can be used. The different values of QRS duration shown in the review are 46.4 ms, 55 ms, 63 ms, 56 ms, 52 ms, 76 ms and 53 ms.

Another interesting finding of the literature study was that when there is a recording with an FSE and a skin electrode placed on the mother's thigh, only the FECG will display a P-wave [22, 23]. In this case, the maternal P-wave will not have enough strength to reach the maternal skin electrode on the thigh and therefore it will not be displayed in the ECG. Furthermore, a recent study suggests that repetitive accelerations during contractions in the case that are above 20 beats per minute (bpm) should be thought as MHR until it is proven is not [23].

In addition, another discovery while searching information about the misidentification of MHR as fetal, was the difference between the bpm [23]. The normal baseline rate for a fetus is between 110 and 160 bpm and for the mother is between 60 and 100 bpm. Even though this is valuable information that could be used to distinguish between the fetal and maternal HR, it is not the best approach. In complicated cases

e.g. due to dehydration, fever or anemia of the mother, it may not be clear what it is MHR or FHR [24]. Also, the fetus could have an unusual HR that could overlap with the maternal one and therefore disregard an important event that needed attention.

Regarding paediatric ECG, the cardiac intervals are different depending on the age [25]. In particular, the conduction intervals such as PR interval and QRS duration are shorter for fetuses when comparing them to adults because of the smaller cardiac size. A table showing the different QRS duration depending of the age can be seen in Table 2.1. It can be observed that the QRS duration for children is mostly below 80 ms.

	0-1 month	1-6 month	6-12 month	1-3 year	3-8 year	8-12 year	12-16 year	Adult
QRS (ms)	50 (70)	50 (70)	50 (70)	60 (70)	70 (80)	70 (90)	70 (100)	80 (100)

**Table 2.1:** QRS duration (ms) as Average (and Upper limit of Normal) [25]

Also to note that there is a difference in the ECG between pregnant and non-pregnant women: a leftward QRS axis deviation may occur which will affect the width of the perceived R-peak and whether the Q and S peaks are visible or not [26]. This is due that the organs in the body move due to pregnancy.

In addition, there is a difference between males and females regarding the QRS duration [27]. In healthy Caucasians, the mean QRS duration for young (18-29 years) males was 96.4 ms and for young (18-29 years) females 87.7 ms and this disparity is preserved during the years. Furthermore, the QRS duration measurement may vary between different ECG machines and their approach in how to calculate it. For instance, one software calculated the average QRS duration in 423 women as 80 ms and another with the same data got the result of 91 ms. The same software applied to 377 males gave 90 and 95 ms respectively.

In the same way for men and women, the QRS duration increases from birth to the incoming years [27]. However, the QRS duration for males becomes larger after adolescence and that disparity is still there after correcting for body and cardiac mass [28]. As a result of the large difference after adolescence, it is believed that sex hormones affect the cardiac intervals. Studies with animals have shown that sex hormones such as estrogen, progesterone and testosterone modify the QTc interval: estrogen increases it while testosterone and progesterone shorten it. There is no data if the sex of the fetus affects the cardiac intervals but since it is not that significant before puberty the differences should be minimal.

To summarize the most important outcomes of the literature study and that were applied to the implementation of the algorithm. These outcomes aimed to solve the challenge of differentiating between maternal and fetal beat. First, when a thigh

## 2. Theory

---

electrode is used on the mother together with the FSE, the P-wave of the mother will not be displayed since it does not have enough strength. In the case that there is no P-wave, the MHR will be picked and it could be applied to disregard the beat or apply a bad score to the beat. Secondly, the QRS duration varies depending of the cardiac size and due to that reason it can be used to distinguish between the FECG and MECG and act accordingly.

# 3

## Methods

This chapter describes the tools and data that were utilized for the development of this project. The data sets were used to investigate the characteristics of the peak such as the QRS width and the occurrence of P-wave and to draw conclusions from them. In addition, this chapter describes the design of the algorithm which is divided in the common parts of it, as well as an approach taken for the QRS width based on the literature study and another approach taken for the QRS width based on statistics.

### 3.1 Tools

*Raw data viewer* was used to analyze the raw data files (.dsp) that were collected for years in hospitals and contain FECG leads in 500Hz resolution. This tool allows to observe different leads and can zoom in or out in the amplitude levels as well as modify how many seconds of data are being shown. A picture of the tool can be seen in Figure 3.1.

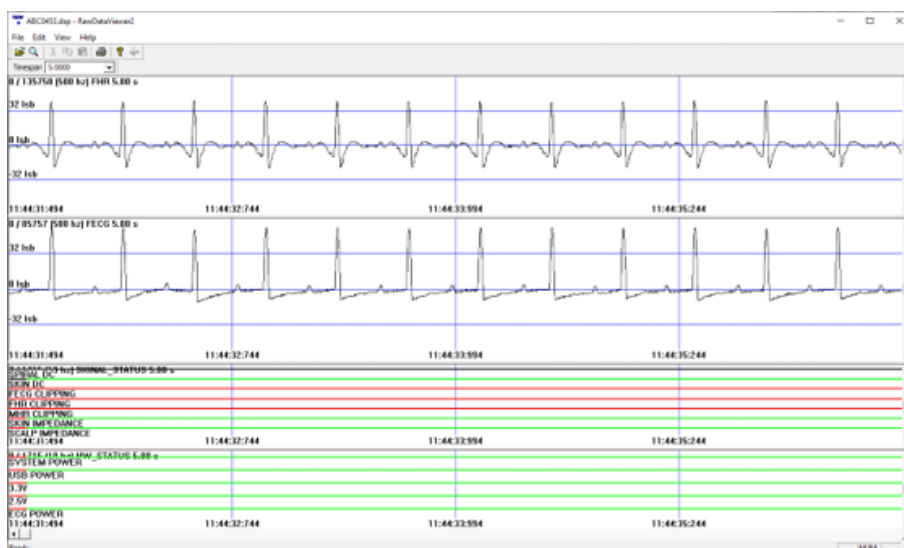


Figure 3.1: Raw Data Viewer

The main algorithm and product of Neoventa outputs a file in STN or STF format which the program *Stan Viewer* can visualize. This tool is used by customers, clinicians and developers for reviewing the output recordings.

### 3. Methods

Moreover, this program was used in this thesis to study the output quality of the new approach. A picture of version 2 of *Stan Viewer* can be seen in Figure 3.2 and one of version 3 in Figure 3.3.

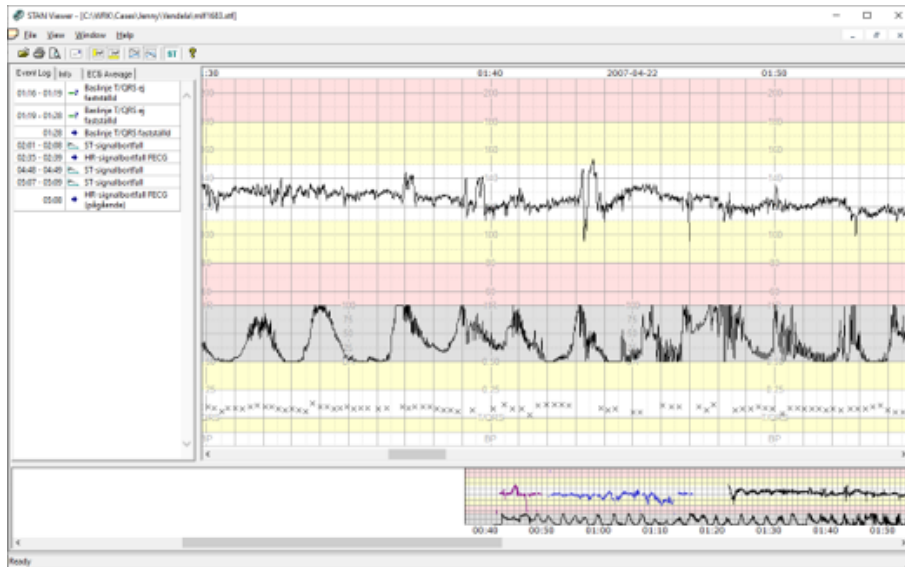


Figure 3.2: Stan Viewer 2

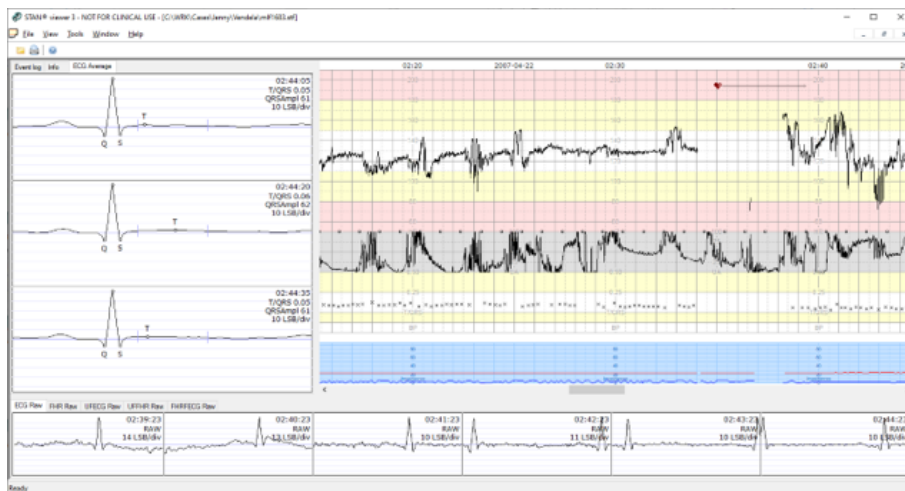


Figure 3.3: Stan Viewer 3

A useful tool for this project was the *STN Diagnostics* which creates a spreadsheet with a number of measures for each STN recording file in a data set. An image of the tool can be seen in Figure 3.4. In addition, an image showing an example of the spreadsheet output can be seen in Figure 3.5.



### 3. Methods

The tool can be used to compare different sites, algorithms and other parameters. Since there is the possibility of adding new measures to be studied, some parameters of the P-wave were researched. The parameters that were studied about the P-wave are the mean, the amount of waves per recording, minimum, maximum, median, 20% percentile, 40% percentile, 60% percentile, 80% percentile, 95% percentile and 97% percentile. Histograms of all these values per recording can be seen in Figure 3.6, Figure A.1, Figure A.2, Figure A.3, Figure A.4, Figure A.5, Figure A.6, Figure A.7, Figure A.8, Figure A.9, Figure A.10, Figure A.11 and Figure A.12.

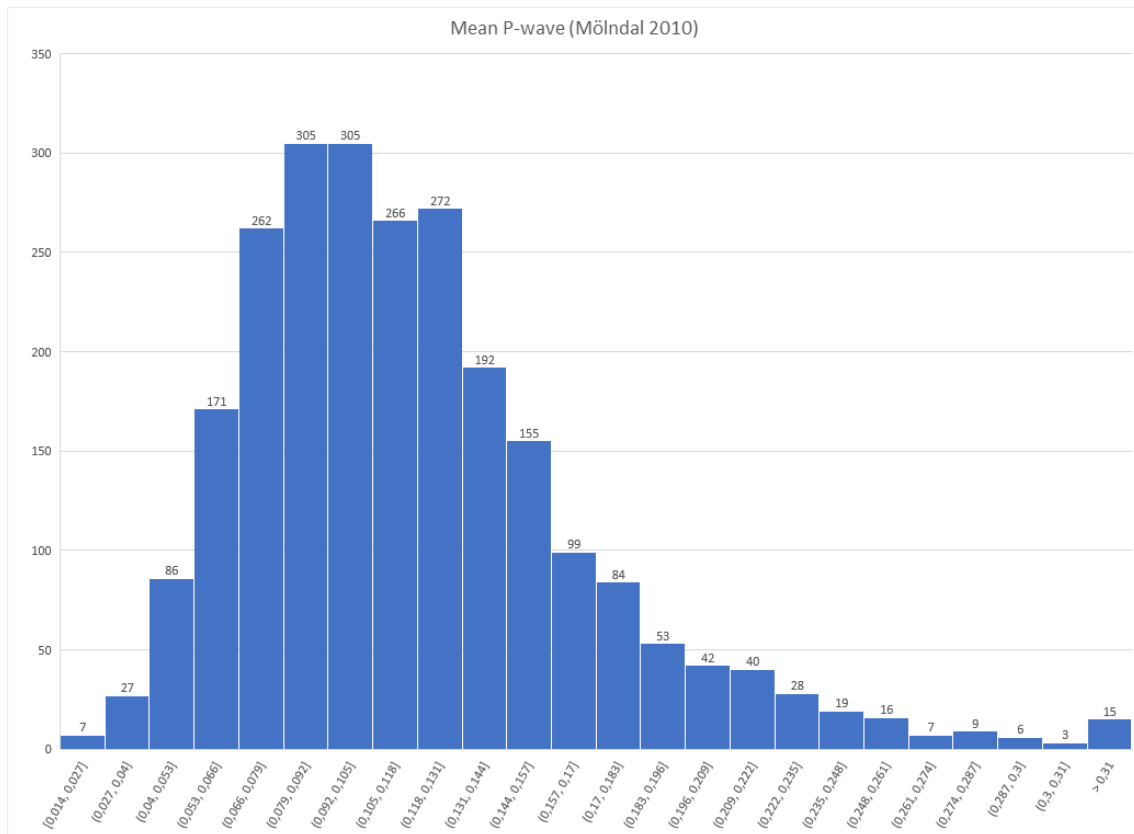


**Figure 3.6:** Histogram of the mean value of the P-wave (round 3 decimals)

Furthermore, another tool called *Recording Details* was used as a way of reviewing an STN file in a detailed level which was primarily used for troubleshooting, the tool can also give a spreadsheet output similar to *STN Diagnostics*. A picture of the *Recording Details* tool can be seen in Figure 3.7.

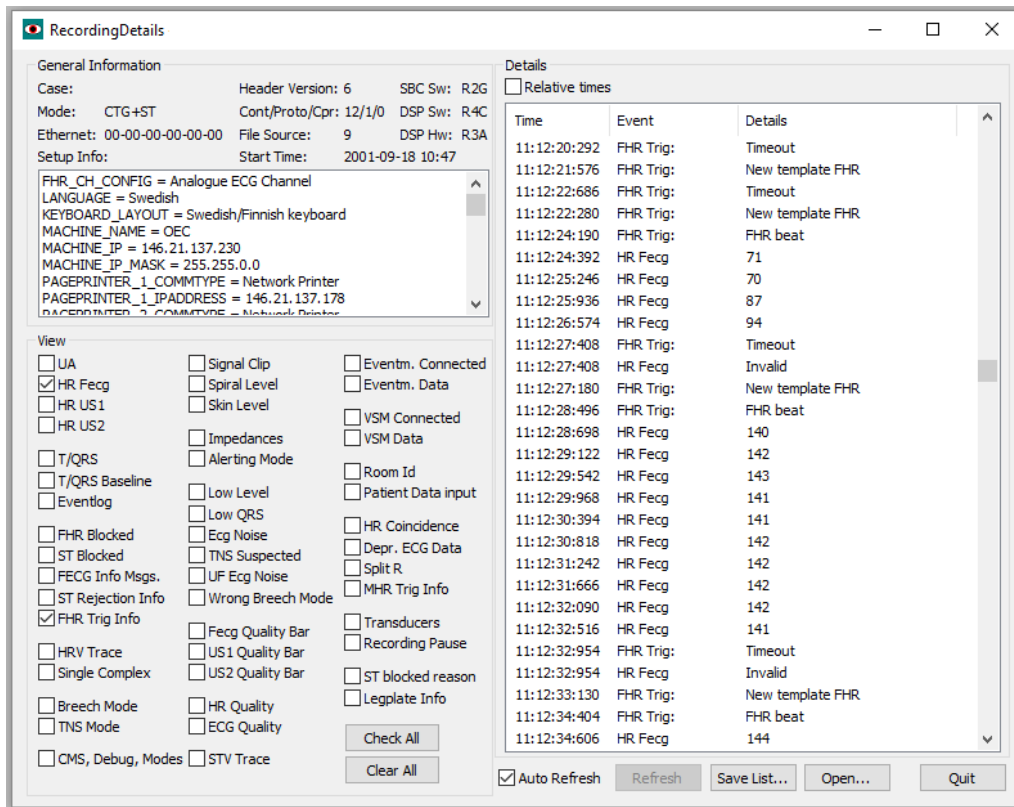


Figure 3.7: Recording Details tool

## 3.2 Data

First, some specific files with occurrences of maternal beats being presented as fetal beats and consequently being the base to calculate the HR and FECCG parameters were used for the development of the code.

One quality measurements that was used to evaluate if the algorithm was improving or not is to count how many FECCG HR are below 100 bpm from the output of the recording details. This measurement is useful since the FHR should not be in that range and if that value is appearing it is because the MHR is being presented as FHR [29].

Another measurement is how many HR are being displayed. This is useful to know because in the case that the chosen template was wrong, the algorithm wastes valuable time searching for matches. This will discard the template and the algorithm will search for a new one again. Also, it will prevent the HR from being displayed. In addition, it is useful to know how much of the percentage is below of 100 having to know how much this value affects the total.

Furthermore, the variability refers to FECCG FHR variability measurement provided by the tool which is related of how much the HR is changing from value to value. In the case that it is known that there are maternal beats presented as fetal beats,

the variability might give a higher value than what it actually is. For that reason and while evaluating the results, a lower average variability indicates less false beats which is a positive outcome.

In addition, HR Coverage quality refers to the HR FECG coverage which is based on the connected FECG per patient and is the time in which the FSE is connected. This value shows how much percentage during the time the electrode has been connected is actually being displayed in the tool, being the value 100% the best possible.

The dataset used for evaluating the improvement of the new approach were a subset of the raw data files collected with STAN S21 and S31 around 2010 in a Swedish hospital which in this report is referred as the Neoventa database. The raw data files consists of recordings during labour.

This dataset was also used for statistical purposes to retrieve important characteristics of the fetal heart beats that were useful to apply in the design of the algorithm. In Table 3.1, the amount of files and hours used for the evaluation of the algorithm is shown. The amount of total files used was 3560 having a total of 10068 hours, 53 minutes and 54 seconds of recordings. The time format is displayed as hours first, then minutes and last seconds.

	Files used	Recording hours
Q1; S21	131	343:22:44
Q1; S31	898	2543:38:19
Q2; S21	112	313:12:12
Q2; S31	916	2598:16:09
Q3; S21	93	280:48:55
Q3; S31	752	2071:12:48
Q4; S21	104	324:39:21
Q4; S31	554	1593:43:26
Total	3560	10068:53:54

**Table 3.1:** Amount of files used and hours of recording from the Neoventa database

Furthermore, the raw data files are the input used in the STAN fetal monitor (also the code modified in this thesis) which outputs the recording files STN or STF that are collected for every recording made at a customer site. This is also the format that is used internally for testing the algorithms.

In addition, there was a high amount of raw data files with unexplored data which most likely contained a few cases with partial MHR presented as FHR. However, it is not possible to look through these files manually with the raw data viewer since it would have been high time consuming and challenging to identify the maternal beat. Nonetheless, comparing the differences between the new and old design coverage, new problematic files could be found to improve the algorithm in the future.

### 3.3 Design of the algorithm

As a result of the outcomes of the literature study and the analysis of the previously specified data, several approaches for an algorithm design were discussed for discerning a maternal beat from a fetal occurrence.

A general idea of what the algorithm does: first, the algorithm looks at a 2000ms long segment of data. Then, it finds the ECG beats and then scores them to single out the last of the fetal beats, while discriminating maternal beats and (possibly) artificial beats originating from interference from nearby devices.

From the literature study, one of the two main outcomes was to use the location of the P-wave to determine if the beat is maternal or fetal. However, the other outcome is regarding the duration of the QRS complex and will be one of the main focuses of the algorithm. Other quality measurements were also performed such as the difference between the current and previous sample during a window of time, this is made to discard noisy signals.

The algorithm developed has several parts that are interesting to be shown. The following sections are divided in the common parts of the algorithm and the different approaches taken in the measurement of the QRS width. The design of the algorithm consists of scoring different features of the peak detected and gives a final total score of the specific peak. Then, the peak with the highest score is chosen as a possible template. However, the peak chosen could still be rejected as an acceptable template if it does not fulfill the quality measures.

#### 3.3.1 Common sections

First, a set of the 15 highest values in an interval of 2 seconds is found. The motivation behind choosing 15 peaks was due to trial and error with the output results and finding a good balance between finding all the interesting peaks and efficiency. However, this part will be explained in more detail in section 5.5.

These maximums are considered the peaks in this period of time. The peaks have a protection around them of what is considered the template size on the left and right side. This is so the peaks are not too close to each other and to avoid that the picked value is not part of the same beat.

Giving the position where the peak is located, the score of the position is calculated. The closer the position is to the end, the higher the score should be. The reason behind this is in the selection interval of 2 seconds it is likely to be several beats from the same source (fetal and maternal). In addition, due to the construction of the beat detection algorithm it is needed to pinpoint the latest one. Also, the limits used to give more score are based in the maximum FHR possible which be circa 200 bpm in case of fetal tachycardia, an approximate limit of this is around 240 bpm [30]. If 240 bpm is calculated to ms, it gives an interval of 250 ms between peaks.

This means that a peak in the last 250ms of the window is more likely to be a fetal beat and should be given preference.

Different approaches were tested giving more decimals or rounded scores to the position score. The approach that was decided to be used is a step function at the beginning and at the end of the interval with a slope in the middle of the range, as it can be seen in Figure 3.8. The slope interval is calculated based on the formula in Equation 3.1.

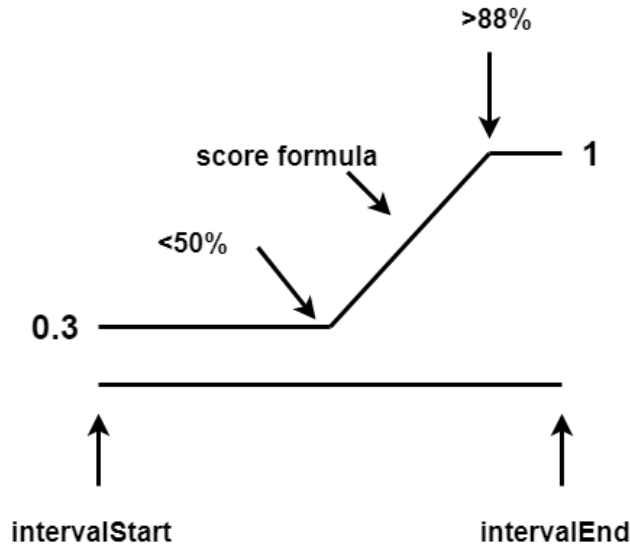


**Figure 3.8:** Score position used

$$\text{Score position} = 1 + \frac{\text{pos} - \text{intervalEnd} + 1}{\text{intervalEnd} - \text{intervalStart}} \quad (3.1)$$

Different approaches were made regarding the amplitude of the peak. One approach that was tested was if the amplitude of the peak is between 10 and 150 least significant bit (lsb), a higher score was given. It means that if the amplitude is between 10 and 150 it is in the range of a fetal beat that ranges between 50 $\mu$ V and 750 $\mu$ V since 1 lsb is equal to 5 $\mu$ V.

A histogram that shows the range of amplitudes for the fetal beat can be seen in Figure 3.9. Otherwise, outside of this range, it was given a lower score since it is still useful to not reject beats with low amplitude. However, it was found out that this approach would discriminate fetal beats that had a too small amplitude. For that reason, in case that there is a peak the score is always one. This will be discussed in more detail in section 5.1.

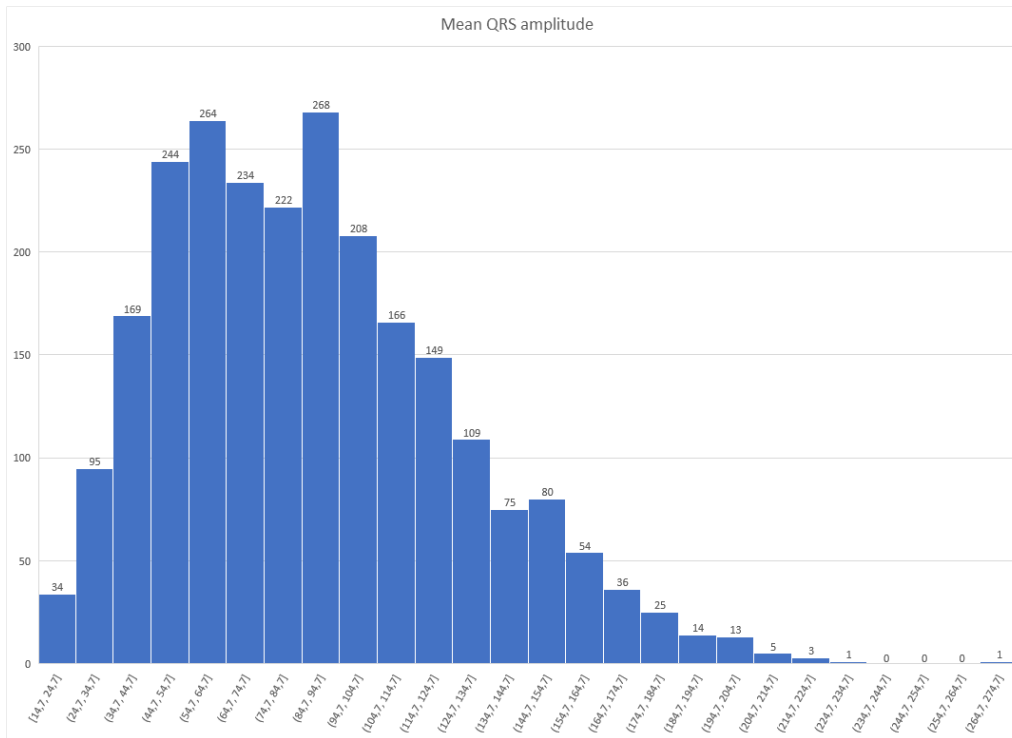


**Figure 3.9:** Histogram of the QRS amplitude with one year data of the database

Furthermore, a measurement for giving a score to the shape was done as well. This is useful to discard signals that are too noisy and/or have high amount of notches. Two procedures were tested for this purpose. One was the standard definition of energy of a signal (see Equation 3.2). The second procedure and formula used to rate the shape was based on the summation of the difference of the current and previous value as seen in Equation 3.3 over the template width, as well as to normalize the signal given the amplitude of the peak. Due to that, the result value is the mean value of the consecutive difference.

$$E = \frac{1}{N} \sum_{n=-\text{Template size}}^{\text{Template size}} |s_n^2| \quad (3.2)$$

$$E = \frac{1}{N} \sum_{n=-\text{Template size}}^{\text{Template size}} |s_n - s_{n-1}| \quad (3.3)$$

The second approach was the one decided to be used since it was a more relevant formula than just the energy itself since it is more significant to identify the differences in the signal. To support the decision of which thresholds to be used in the code, statistics about the mean difference between consecutive values in the Neoventa database were run. A histogram of this can be seen in Figure 3.10. As said before, this approach helps to discriminate noisy signals. Next, this value is checked: if it is below the threshold specified, which in the algorithm coded was 0.3 and deduced from the statistics, the score of one is given.

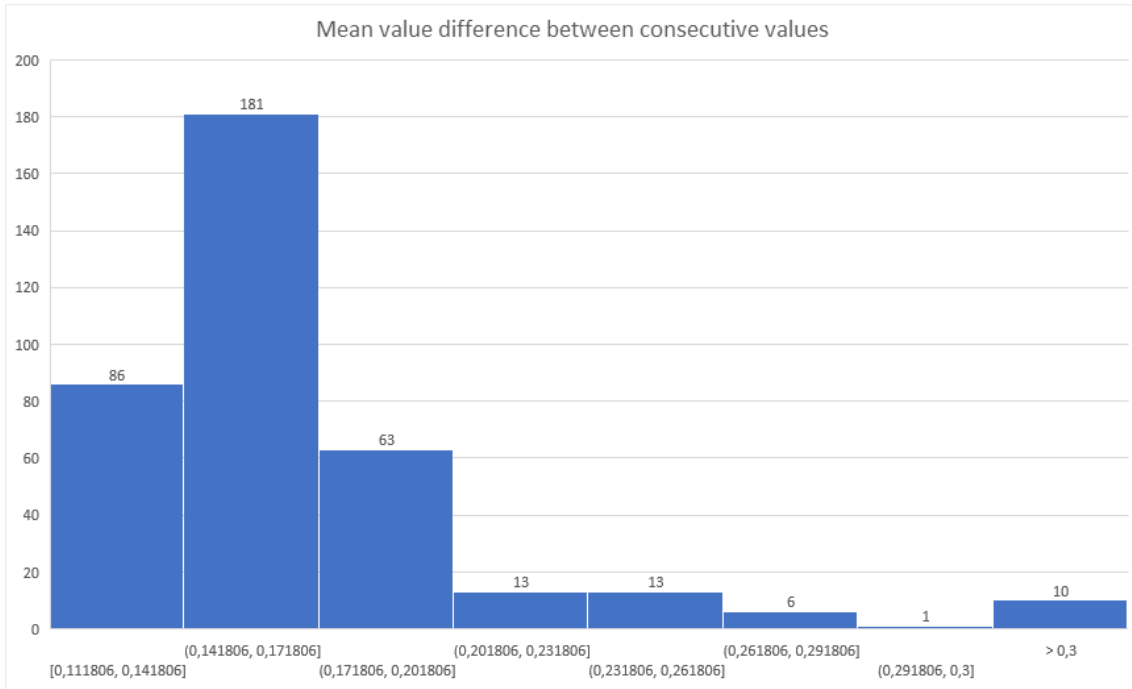


**Figure 3.10:** Histogram of the output of Equation 3.3

Regarding the P-shape, since the position of P-wave is known relatively of the position of the peak as a set of global variables, these variables were used to loop from the start of the P-wave until end of it. The mean P-wave value is calculated and if it is more or equal than 0.079 the score of one is given. Otherwise, no score is given. This score is useful since it was discovered in the literature study that an absence of the P-wave in a setup with an FSE means that it is more likely to be a maternal beat. A histogram regarding the mean value of the P-wave and the reason behind the threshold used can be seen in Figure 3.6.

Next, when all the individual scores are calculated, it is needed to combine them in a meaningful way. The score of the QRS width is made in two approaches explained in subsection 3.3.2 and subsection 3.3.3. In detail, the score of the amplitude is multiplied by the sum of all the other scores. This is the approach used in case that the peak is more than zero, otherwise no score value is assigned to it. The score of the position, QRS width, shape of the peak and appearance of P-wave all have the same weight. The final formula of the combination of the score can be seen in Equation 3.4

$$\text{Total score} = \text{sAmplitude} * (\text{sPosition} + \text{sQRS} + \text{sShape} + \text{sPwave}) \quad (3.4)$$

Next, when all the scores of the peaks have been calculated individually, the one with the highest score and that has an amplitude different than zero is chosen as the best peak.

Given the best peak, the code was tested using rejection mechanisms or not to study how much it actually affects the peak. However, in the final version of the code the rejection mechanisms were applied to ensure a good quality of the signal and are explained in the next paragraphs.

One quality measurement used in both the original and new approach is to calculate the mean amplitude around the possible template to analyze if there is too much noise around. If the peak is lower than this mean value, the peak is rejected. Also, the peak is rejected if its amplitude is not twice as large as the highest peak outside of the same boundaries calculated for the mean value. Both rejection mechanisms are useful to be more robust against noise but they also have some drawbacks that will be discussed in chapter 4.

Another rejection mechanism was used which is that if the amplitude of the peak is higher than a maximum specified in the code, the peak is rejected. In detail, the value used in the code was 400 lsb. As well as reject the peak if there is no score assigned to it.

Finally, if the peak has not been rejected, the position of the peak is given to the function that handles the template and applies further rejection mechanism in case that the template is not valid.

### **3.3.2 First approach regarding the width of the QRS complex**

The first approach to give a score to the QRS width was mainly based in the output of the literature study. The method that is used to calculate the QRS duration has two procedures depending on if the peak is positive or negative. For the implementation of this algorithm it was supposed that if the peak is positive it is an R-peak and if it is negative it is an S-peak.

When a positive peak is found, it is needed to know where the position when the Q starts is. The signal is looped in the left direction to find where Q starts. A visualization of the looping can be seen in Figure 3.11.

Next, the difference between the current and previous amplitude position is calculated. If the signal is decreasing, it is tagged. The same is done in case it is increasing. In the individual case of a positive peak and finding the beginning of Q, it is searched if the signal has decreased and increased at least once, as well as if the current difference between the previous and current value is two and also the current value is less or equal than one. If this is true, the position is saved as the start of the Q-segment (see Figure 3.11).

The same procedure is done for selecting the end of the S-peak by looping to the right side of the signal and selecting where the position is. This can be seen in Figure 3.12.

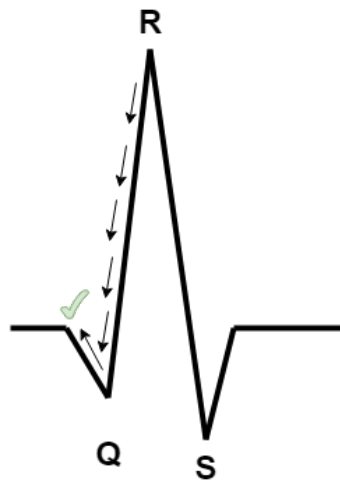


**Figure 3.11:** Loop left side of the R-peak

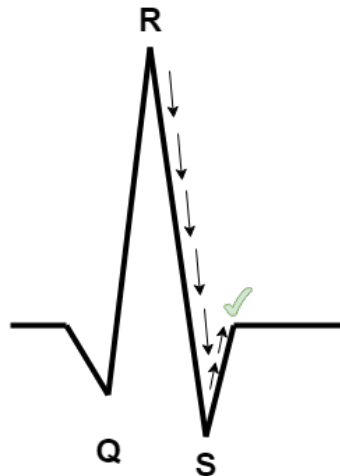


**Figure 3.12:** Loop right side of the R-peak

Another ECG configuration could be when the maximum is an S-peak. In the case that a negative peak is detected, the beginning of the Q segment is found with the combination that the signal has increased two times and decreased once, the difference of the current and previous value is in the range of two and that the current value looped is less or equal one (see Figure 3.13). For finding the end of the S-peak, the approach is that it has only increased substantially once and that the current position is less or equal to one. The procedure can be seen in Figure 3.14.

If the beginning of Q and the end of S have been found, the QRS width can be calculated in milliseconds. This value is checked and given the highest score if it is in the range of a fetal beat that has been found in the literature study. If it is in the range of a maternal (adult) beat, it is given a lower score and if it looks like an artificially generated peak is given a negative score to punish it.

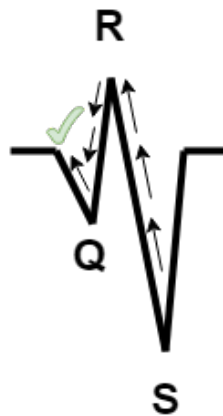


**Figure 3.13:** Loop left side of the S-peak



**Figure 3.14:** Loop right side of the S-peak

As a result of having available statistics of Neoventa, it was known that having beats that only contain qR and Rs could be a possibility. For that reason, in case only the beginning of Q or the end S was found, it was given a score as well to not discriminate these other ECG appearance cases.

### 3.3.3 Second approach regarding the width of the QRS complex

The second approach taken to differentiate between maternal and fetal regarding the QRS width characteristics was a combination of the literature study, statistics of the Neoventa database and study of the data.

From the literature study it was known that the maternal beat has a longer QRS duration than the fetal beat. However, it is challenging to measure the QRS in diverse ECG configurations as multiple configurations which can be seen in section 2.4. Furthermore, there is no data available of what the researchers considered the beginning of Q and the end of S and it may differ between studies [27].

The approach applied in this section is more practical and general than the first approach since the QRS configuration may differ between different recordings or even in the same recording while more time is passing. Since different ECG configurations are common, a more general approach is more useful than coding a procedure for the different configurations, diverse ECG configurations can be seen in section 2.4. Consequently, the first approach is not an optimal solution to measure the QRS duration directly. For that reason, with this approach some of the problems observed in the first approach can be solved.

The common parts in the second approach are the same as in the first approach which are described in subsection 3.3.1. For the purpose to have reliable assumptions on which the algorithm is based, statistics with a quarter of data of the Neoventa database were made and can be seen in Figure 3.16.

The graph shows a histogram of the duration in milliseconds where the peak is half way of its maximum which is illustrated in Figure 3.15. To be clear, the same procedure to calculate the duration in the 50% of the peak is done in the algorithm as for getting statistics of the data.

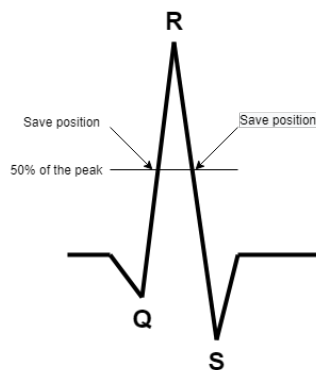


**Figure 3.15:** Width in the 50% duration

The way in which the duration in the 50% of the peak is calculated is when the position of the peak is known. First, it is looped through the left side until a value that is less or equal than the 50% is found as it can be seen in Figure 3.17 and that position is saved. Then the same procedure is done by looping to the right side which can be seen in Figure 3.18.

When both the left and right positions are found, the duration of the peak at this height is measured in samples and converted into milliseconds. Next, if the value previously calculated is more or equal than 6 and less or equal than 20, the maximum score is assigned which corresponds to the value one. This value is assigned since this duration falls in the distribution of the fetal beat range as seen in Figure 3.16.

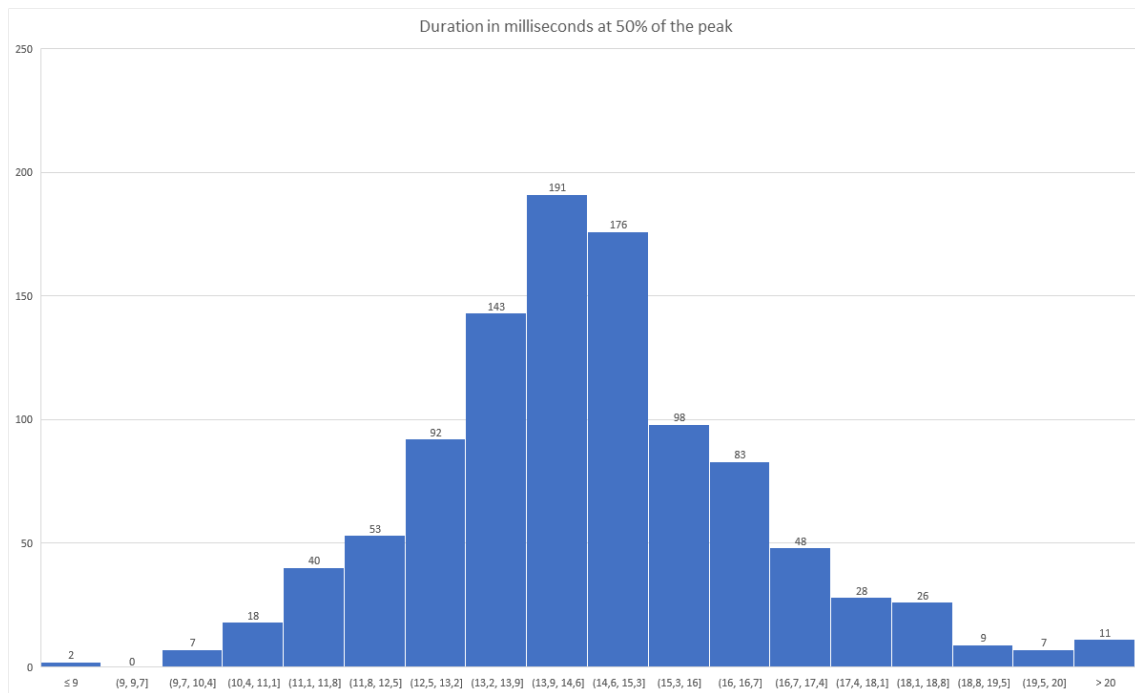


**Figure 3.16:** Histogram of the width in the 50% part of the peak

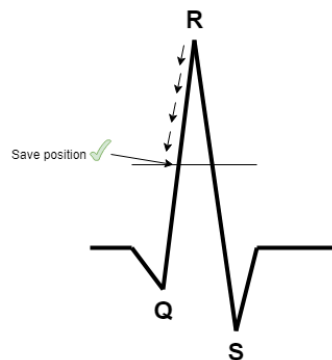


**Figure 3.17:** Looping left to find the position in the 50% duration

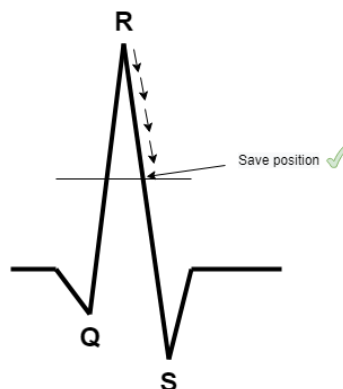


**Figure 3.18:** Looping right to find the position in the 50% duration

### 3. Methods

---

In case the duration falls in the range of being more than 20 and less or equal than 24, the score value is assigned to be 0.9. The reason for this is that the fetal and maternal distribution overlap and it would not be correct to give a much lower score than the maximum since. In the end, it could still be inside the distribution of a fetal beat.

Unfortunately, there is no statistical data available of the maternal beat duration from the Neoventa database. However, manual measurements of the raw data were taken and some examples and the ranges that they fall into can be seen in Figure 3.19, Figure 3.20, Figure 3.21 and Figure 3.22. As it can be seen, the duration of the beat at half of the height are 27 ms, 21 ms, 22 ms and 25 ms respectively. These beats can be identified as maternal beats by experts since the width of the peak can be observed as much wider than the others.

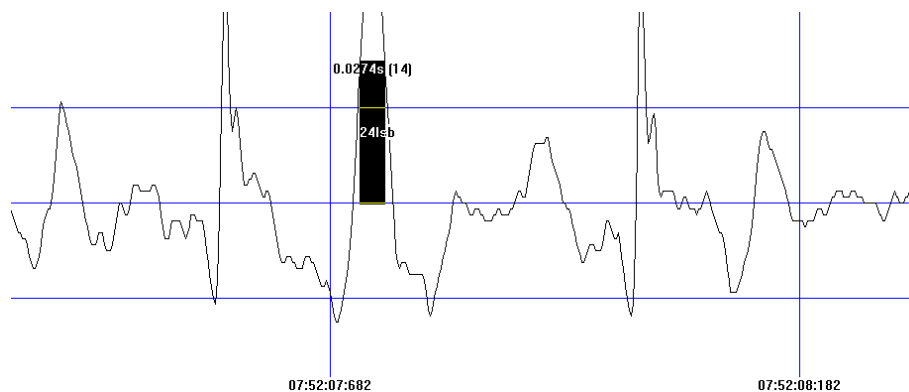


**Figure 3.19:** Example maternal beat 50% width

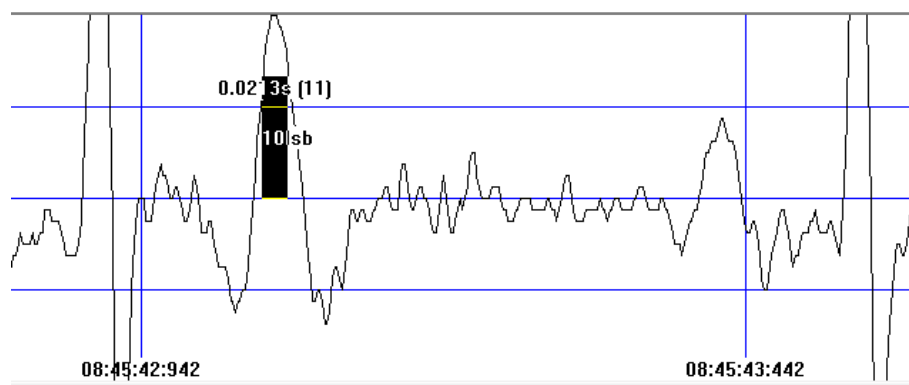


**Figure 3.20:** Example maternal beat 50% width

Also manual measurements of fetal width at 50% of the peak were made and one example can be seen in Figure 3.23.

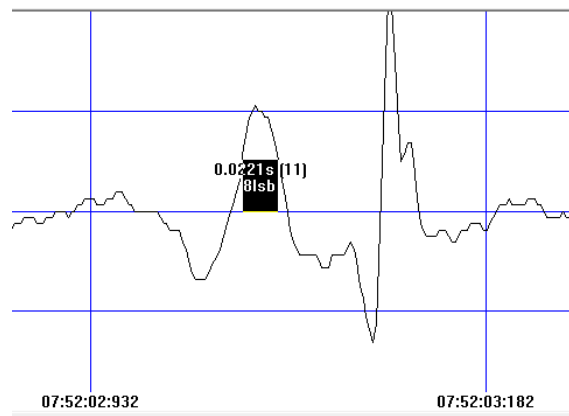


**Figure 3.21:** Example maternal beat 50% width

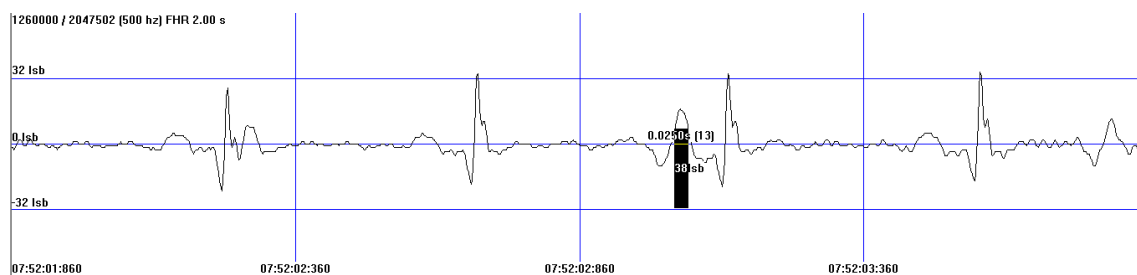


**Figure 3.22:** Example maternal beat 50% width

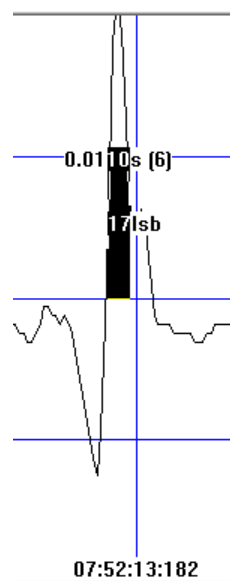


**Figure 3.23:** Example fetal beat 50% width

Furthermore, if the duration value is between more than 24 and less than 40, a value of 0.6 is assigned. This score is chosen much lower because it is unlikely to be a fetal beat. However, even if it is a maternal beat it is not appropriate to reject the beat since the algorithm could be used for testing purposes which not hospitals have FECG simulators and may be using adult ECG versions.

### 3. Methods

---

And finally, if the value is not in any of the ranges previously described and is different than zero, a score of minus one is given. This is to discriminate small peaks that could be artificially noise generated or other maximums that do not fall in any range and are neither fetal nor maternal beats.

# 4

## Results

This chapter is divided in preliminary results and final results made with the Neoventa database. In the preliminary results the original data parameters are presented and compared with the two approaches taken for the QRS width.

### 4.1 Preliminary results

For the development of the algorithm four specific files were used to be studied as preliminary results. The selected data files have occurrences of maternal beat being presented as fetal which is the reason why they were selected to aim to being solved. As explained in chapter 3, the algorithm developed has several parts. The following sections show the results with the different approaches taken in the measurement of the QRS width.

#### 4.1.1 Data used

A table of the results with the original algorithm provided can be seen in Table 4.1 and the preliminary results of the two approaches will be compared with this table.

As it can be seen, the values below 100 HR are 694 (1.76%), 330 (4.53%), 1164 (12.04%) and 150 (1.99%) for 0281, 1331, 1374 and 1294 respectively. The total HR amount displayed are 39080 for 0281, 7286 for 1331, 9666 for 1374 and 7555 for 1294. Regarding the variability the following values were obtained 1.61, 1.09, 2.01 and 1.08 for 0281, 1331, 1374 and 1294 respectively. Respecting the HR coverage quality the values are 93.30%, 89.92%, 92.40%, 88.83% being 0281, 1331, 1374 and 1294 in the same order. A total measurements of the four files was made as well to get an overview of how the algorithm affected all the files. The total amount of values below 100 HR was 2338 being the 3.68% of the total HR of 63587. Furthermore, a total variability of 5.79 and an average of 91.11% of the coverage.

The different parameters used will be studied to evaluate if the several approaches have improved or worsen the output of the algorithm. The quality of the output files is discussed in chapter 5.

	Values below 100HR	Total HR	Variability	HR Coverage Quality
0281	694 (1.76%)	39080	1.61	93.30%
1331	330 (4.53%)	7286	1.09	89.92%
1374	1164 (12.04%)	9666	2.01	92.40%
1294	150 (1.99%)	7555	1.08	88.83%
Total	2338 (3.68%)	63587	5.79	91.11% (avg)

**Table 4.1:** Original algorithm results

### 4.1.2 First approach regarding the width of the QRS complex

The first approach regarding width of the QRS complex has some challenges and problems that were encountered through the implementation of the algorithm. Therefore another approach was considered and will be explained in detail in chapter 5.

There were two tests performed with the different data files. One test was to perform the first approach with rejection mechanism to ensure the equality of the signal that will consequently also ensure the quality of the ST-analysis and can be seen in Table 4.2. The other test was performing the first approach without any kind of rejection mechanism and relying on the score to chose the correct template and can be seen in Table 4.3. The reason why it was interesting to study the results without the rejection mechanism was to observe how much the quality measures limit the choosing of the template with the scores. It can be observed that some files have improved while others got a worse result as they can be seen in Table 4.2 and Table 4.3 compared with Table 4.1.

Regarding the test with rejection mechanism it can be seen in the Table 4.2 that the files 0281, 1331, 1294 improved regarding the amount below 100 HR. On the other hand, 1374 got worse results which can indicate that the rejection mechanism is limiting the algorithm. In addition, the amount of HR values has decreased in 0281 and 1331 but increased in 1374 and 1294. However, none of these numbers were a significant change. Furthermore, the variability got better in 1331 and 1293 but worse in 0281 and 1374. Lower variability is referred to as better in this specific case because it is known that there are appearances of maternal beat being presented and fetal beat which makes the variability to artificially be higher of what it is in reality. Also, the HR coverage quality has improved in 1374 and 1294 but worsened in 0281 and 1331. To sum up, performing an average of the quality, this approach has improved it by 0.20%.

The stf output of the files can be seen in Figure 4.1, Figure 4.2, Figure 4.3 and Figure 4.4. In every picture, the top image is the original output and the bottom is the specific file of this result. It can be seen that FHR spikes in the result files have decreased which is beneficial. In some files the amount of FHR signal loss FECCG has diminished as well.

	Values below 100HR	Total HR	Variability	HR Coverage Quality
0281	651 (1.67%)	39026	1.67	93.14%
1331	9 (0.12%)	7256	0.99	86.95%
1374	1170 (12.03%)	9727	2.11	93.74%
1294	101 (1.30%)	7781	0.89	90.99%
Total	1931 (3.03%)	63790	5.66	91.21% (avg)

Table 4.2: First approach with rejection algorithm results

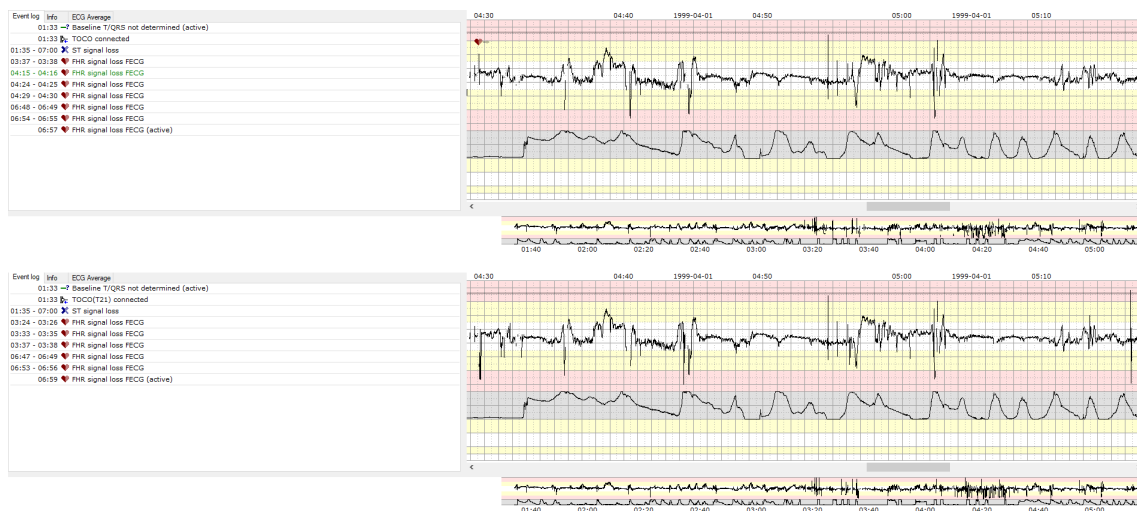


Figure 4.1: 0281 output of the first approach with rejection

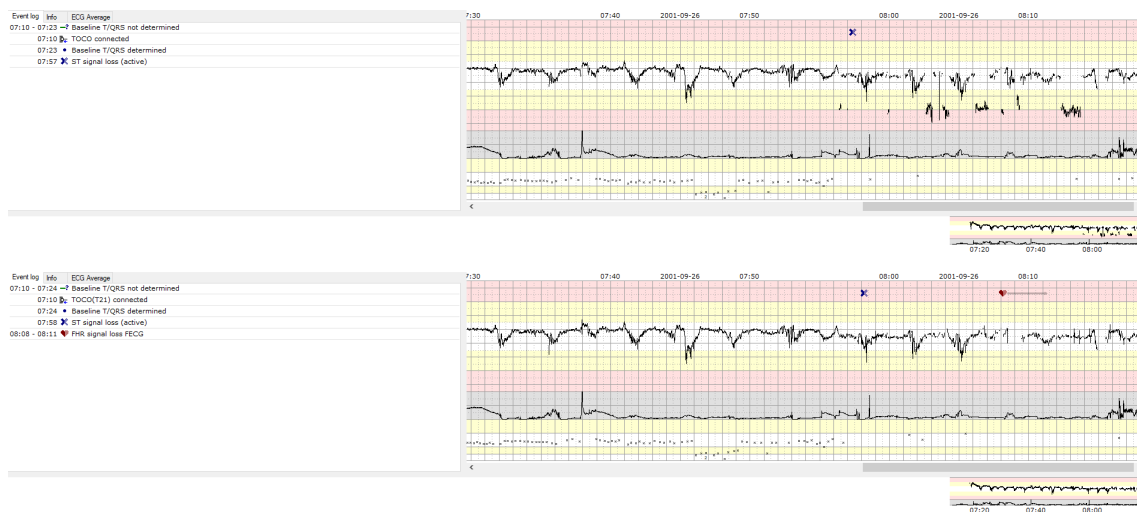


Figure 4.2: 1331 output of the first approach with rejection

## 4. Results

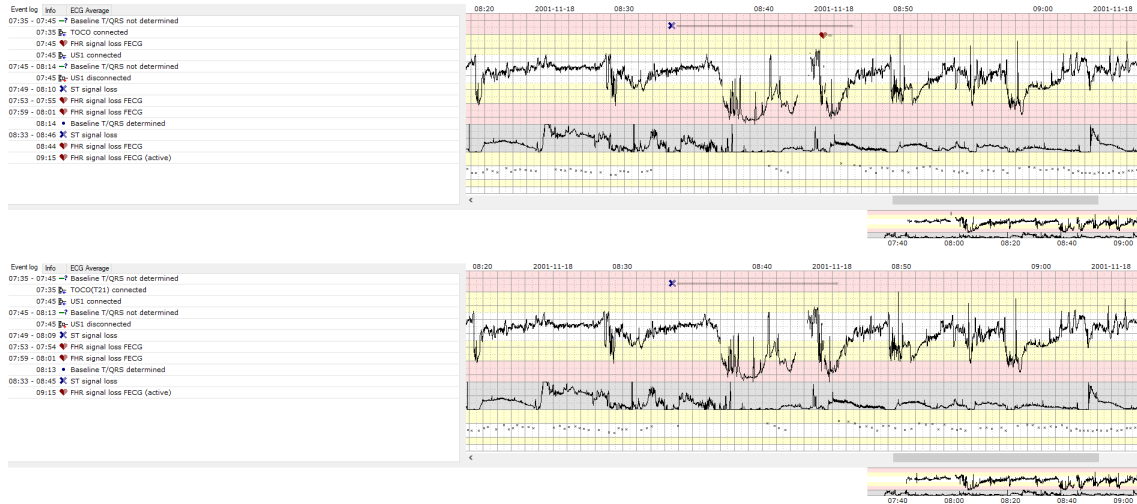


Figure 4.3: 1374 output of the first approach with rejection

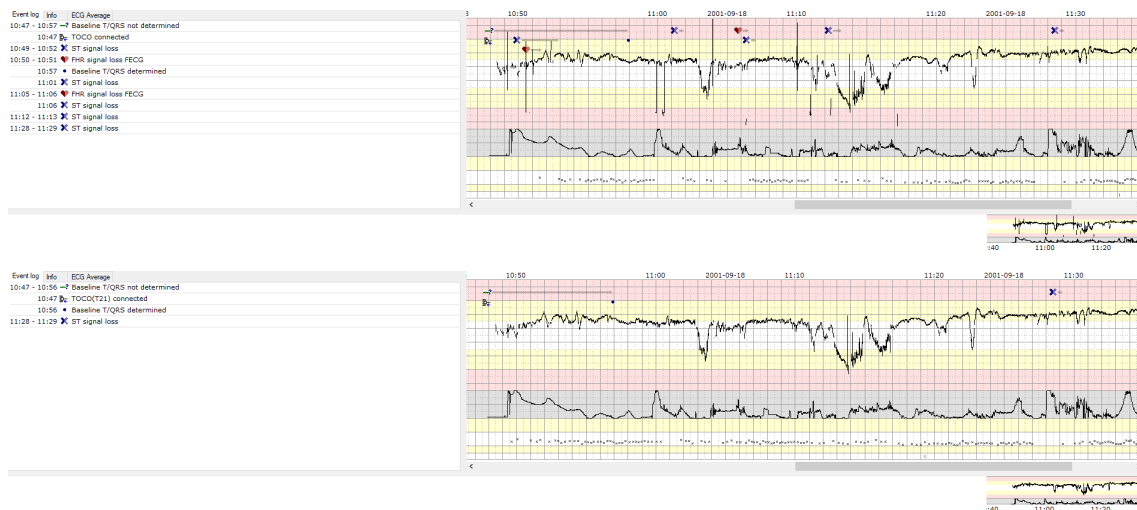


Figure 4.4: 1294 output of the first approach with rejection

Regarding to the test with no rejection mechanism in Table 4.3, all the files besides 1294 have improved the original algorithm and the first approach with no rejection. While 1294 has still improved compared to the first algorithm, it did not for the first approach with rejection.

The most significant change is that the total HR has decreased considerably. This is important to note because the algorithm is using valuable time trying to correlate with a wrong template which makes it lose 2 seconds if it is the case that it does not find any new beat. The variability has decreased in all the files compared to the original algorithm. However, all the files decreased in coverage quality having an average decline of 9.35%.

	Values below 100HR	Total HR	Variability	HR Coverage Quality
0281	419 (1.16%)	35988	1.52	87.73%
1331	28 (0.44%)	6294	0.98	75.11%
1374	1129 (11.92%)	9475	2	92.21%
1294	103 (1.78%)	5793	0.92	71.98%
Total	1679 (2.91%)	57550	5.42	81.76% (avg)

**Table 4.3:** First approach with no rejection algorithm results

To summarize, this test shows us that there is potential to modify the rejection mechanism to find a trade-off between avoiding the maternal peak and choosing the correct template to not lose quality coverage. The stf output of the files can be seen in Figure 4.5, Figure 4.6, Figure 4.7 and Figure 4.8 being the output from the top the original and the one of the bottom the result of this approach. It can be seen that even if there are less noisy spikes in the stf outputs, the FHR signal loss FECCG have increased which is not an optimal result.

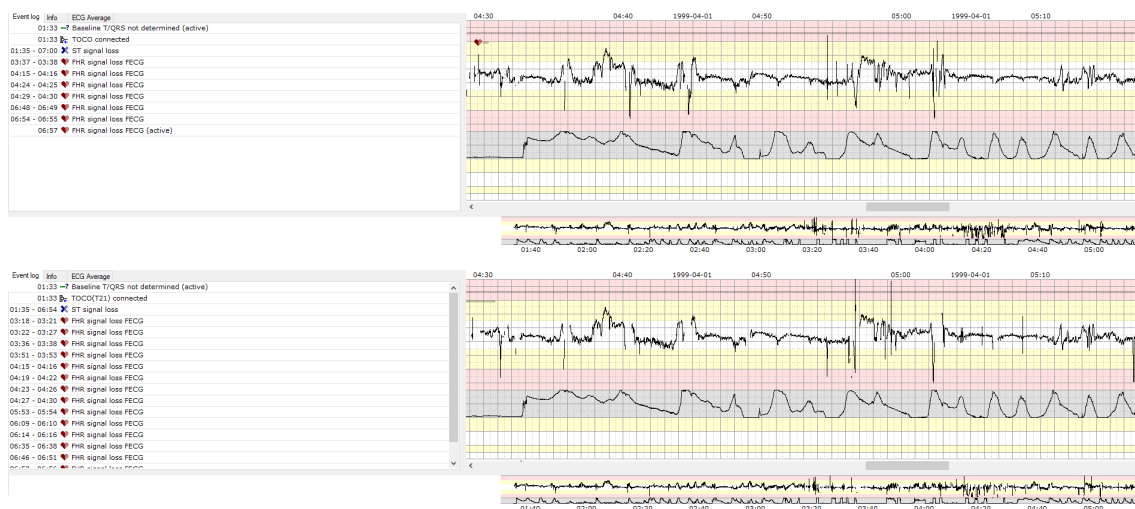


**Figure 4.5:** 0281 output of the first approach with no rejection

## 4. Results



Figure 4.6: 1331 output of the first approach with no rejection

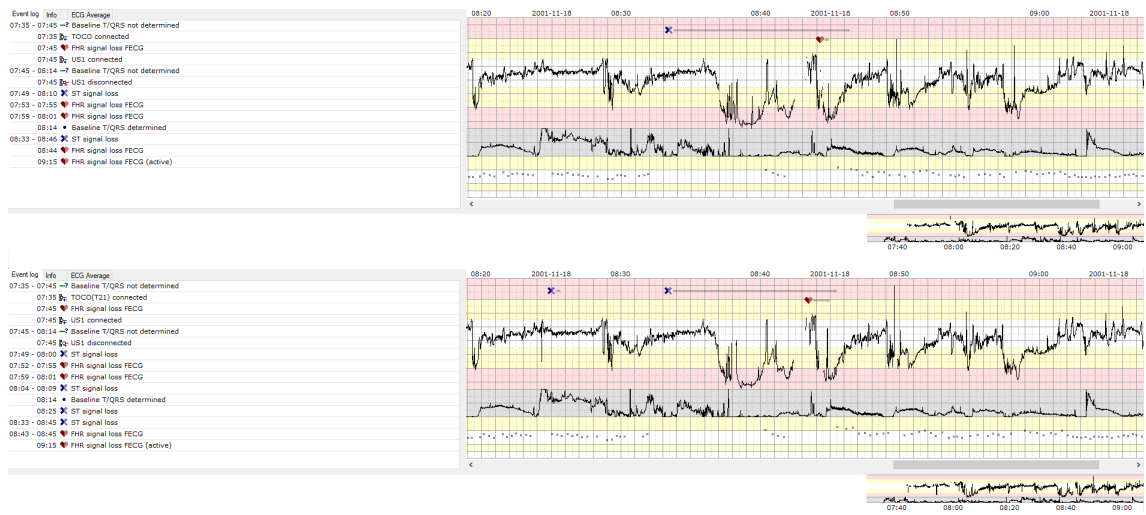


Figure 4.7: 1374 output of the first approach with no rejection

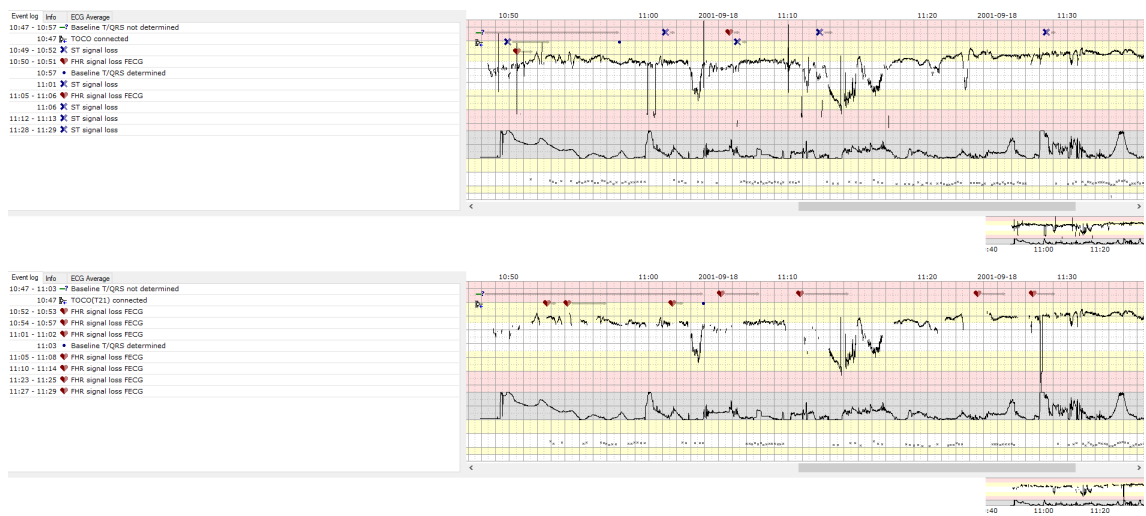


Figure 4.8: 1294 output of the first approach with no rejection

### 4.1.3 Second approach regarding the width of the QRS complex

The results applying the second approach with rejection can be seen in Table 4.4. All files besides 1374 have improved the amount of values below 100 HR. As commented previously it may be because the rejection mechanisms are limiting the chosen template. Regarding the total amount of HR, 1374 and 1294 have increased while 0281 and 1331 have decreased. In addition, the variability has increased in 0281 and 1374 while decreasing in 1331 and 1294. Also, the HR coverage quality stayed almost the same in 0281, decreasing in 1331 and improved in 1374 and 1294, giving an average improvement of 0.48%.

	Values below 100HR	Total HR	Variability	HR Coverage Quality
0281	512 (1.32%)	38856	1.65	93.29%
1331	17 (0.23%)	7397	1.01	88.74%
1374	1170 (12.04%)	9717	2.09	93.85%
1294	99 (1.28%)	7741	0.9	90.47%
Total	1798 (2.82%)	63711	5.65	91.59% (avg)

**Table 4.4:** Second approach with rejection algorithm results

The stf output of the files can be seen in Figure 4.9, Figure 4.10, Figure 4.11 and Figure 4.12 being the output from the top the original and the one of the bottom the result of this approach. The files appear more clean and with less FHR spikes in the output result. Also, the FHR signal loss FECG and ST signal loss has decreased in general. Specially, 1294 (Figure 4.12) got a good result since all the FHR signal loss FECG have disappeared and the ST signal loss has decreased to only one time.

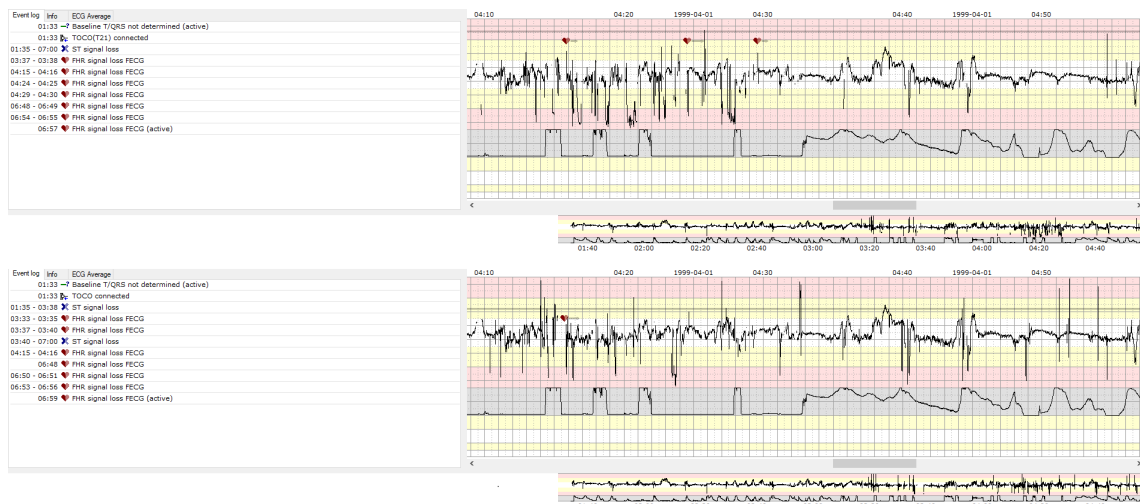


**Figure 4.9:** 0281 output of the second approach with rejection

## 4. Results

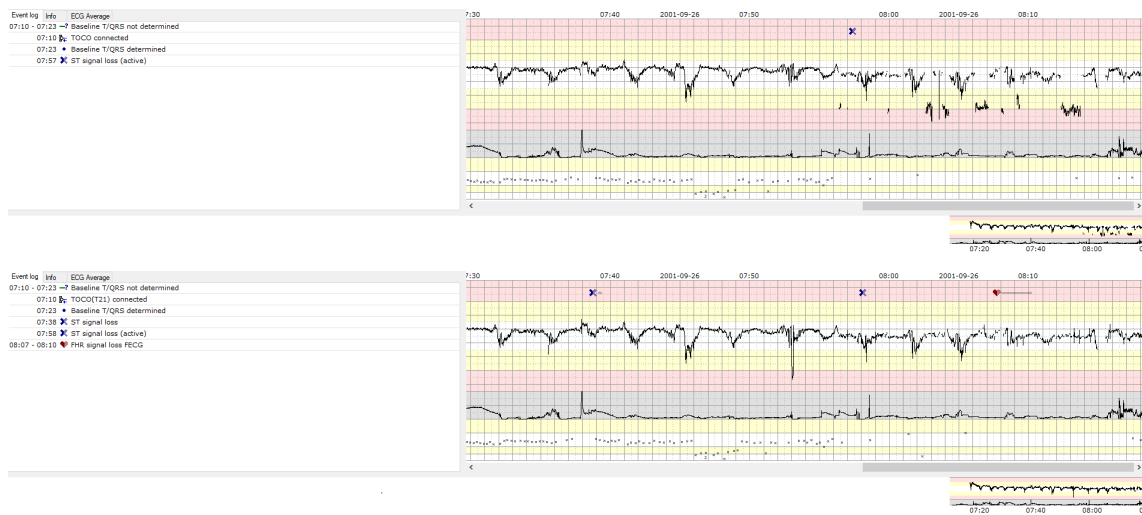


Figure 4.10: 1331 output of the second approach with rejection



Figure 4.11: 1374 output of the second approach with rejection

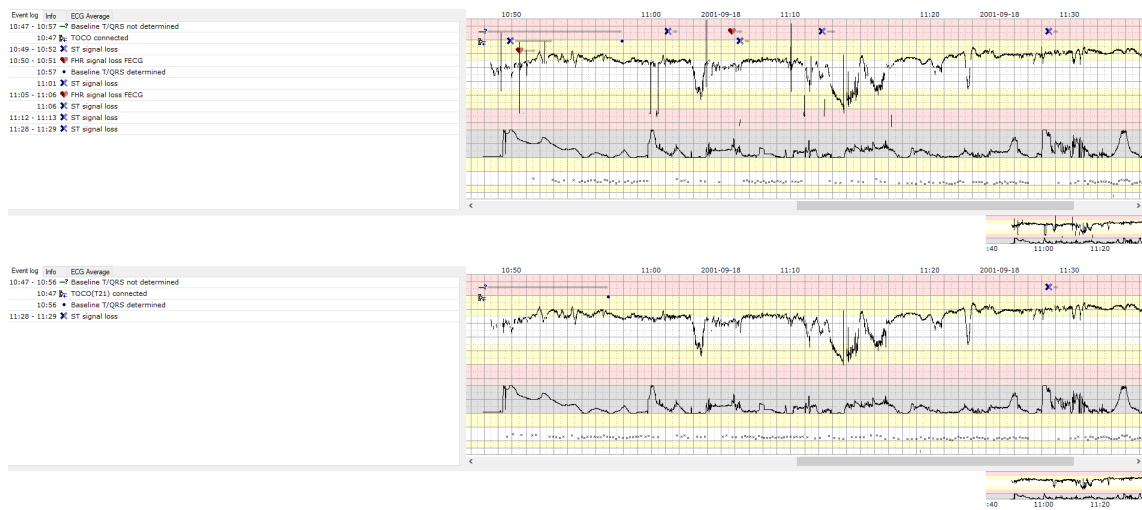


Figure 4.12: 1294 output of the second approach with rejection

The results applying the second approach with no rejection can be seen in Table 4.5. All files besides 0281 have improved the amount of values below 100 HR comparing with the original algorithm. Regarding the total amount of HR, all the files have gotten worse which as it was explained before may mean that the wrong template is getting decided which makes the algorithm waste time looking for similarities, discarding the template and getting a new one. In addition, the variability has decreased in all the files except 1374. Also, the HR coverage quality has decreased in all files, giving an average decrease of 4.38%.

	Values below 100HR	Total HR	Variability	HR Coverage Quality
0281	717 (2.11%)	33964	1.51	86.76%
1331	30 (0.43%)	7017	1.06	84.08%
1374	1140 (11.99%)	9504	2.06	92.35%
1294	8 (0.14%)	5644	0.77	83.74%
Total	1895 (3.38%)	56129	5.4	86.73% (avg)

**Table 4.5:** Second approach with no rejection algorithm results

The stf output of the files can be seen in Figure 4.13, Figure 4.14, Figure 4.15 and Figure 4.16 being the output from the top the original and the one of the bottom the result of this approach. Same as the first approach without no rejection the FHR signal loss FECG has augmented considerably even though some FHR spikes have decreased.

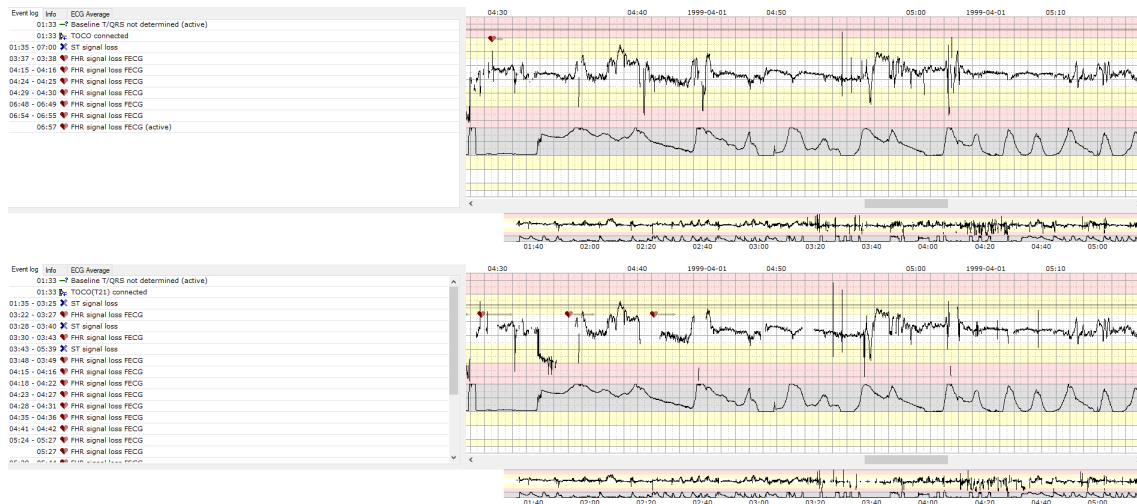


**Figure 4.13:** 0281 output of the second approach with no rejection

## 4. Results

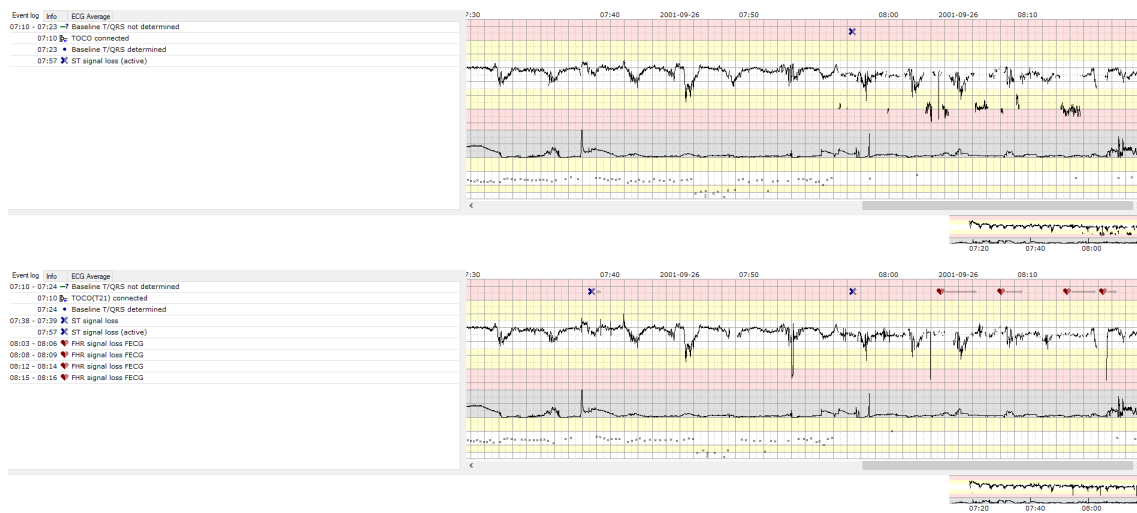


Figure 4.14: 1331 output of the second approach with no rejection



Figure 4.15: 1374 output of the second approach with no rejection

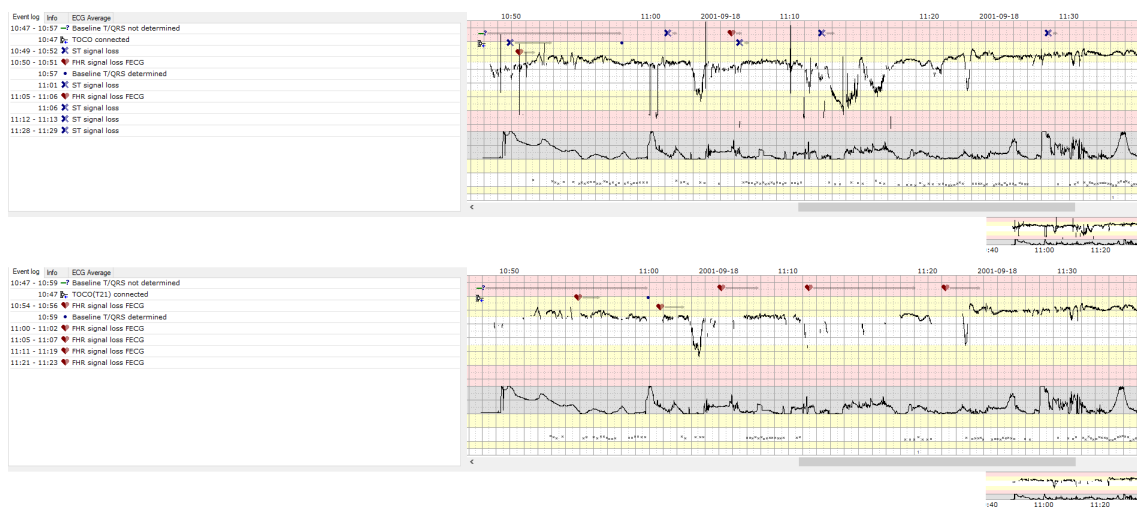


Figure 4.16: 1294 output of the second approach with no rejection

## 4.2 Final results with Neoventa database

The second approach with rejection mechanism and the original algorithm was ran through one year of data to evaluate if the FECG HR coverage quality had improved or declined. The results can be seen in Table 4.6.

	Average difference	Average difference (removing no diff)
Q1; S21	0.08%	0.11%
Q1; S31	0.07%	0.09%
Q2; S21	-0.07%	-0.11%
Q2; S31	0.09%	0.11%
Q3; S21	0.002%	0.002%
Q3; S31	0.15%	0.18%
Q4; S21	0.08%	0.10%
Q4; S31	-0.03%	-0.03%
Total	0.07%	0.09%

**Table 4.6:** Difference between new and old design results with Neoventa database

In the first column of the results called average difference, the average of all the differences between the new result coverage minus the original result coverage is shown. The subset used to evaluate the results were the output files of the *Stn Diagnostics* in which there was an existing value in the HR FECG coverage quality field.

In addition, it was interesting to remove some of the files used in which the output of the new design was exactly the same as the coverage in the old design (which means that the difference between the coverage was zero). This is interesting since these files did not improve or worsen the coverage which may indicate that it is not known for sure if the new code done for this thesis is being used.

The results are divided by quarter and specific machine used during the recording. In two quarters, Q2;S21 and Q4;S31, the average difference has gotten worse (see Table 4.6). It can be seen that in total the new design improves the coverage slightly by 0.07% (see Table 4.6). In particular, when only looking at the results where the output with zero difference is not taken into account, the difference is even greater with an improvement of 0.09%.



# 5

## Discussion

This chapter is divided into an analysis about the common parts of the algorithm with examples of it and an evaluation of the two approaches regarding the QRS width. Furthermore, it also contains a part describing the future work in which this project could be developed further.

### 5.1 Common parts

The most significant change regarding both approaches without rejection mechanisms is that the total HR decreases considerably. The reason behind this is because if the algorithm is trying to correlate with a wrong template, it loses 2 seconds and therefore valuable time.

At the same time, during the development and testing of the algorithm using the rejection mechanism, it was noticed that some parts could be further improved. Unfortunately, a further improvement was out of the scope of this thesis. For that reason, some parts will be discussed in the way that could be improved but not actually implemented.

One common aspect that could be improved is to give a gradual score regarding the amplitude. In the implemented algorithm, the amplitude score is a binary value, which can give edge cases situations where the wrong peak is chosen. An example of this can be seen in Figure 5.1. Here, peak 9 is the wrongly picked. The associated sub-scores can be seen broken down in Table 5.1 and Table 5.2. This problem appears in the second approach since the 50% of the peak in low amplitudes peaks is an extremely low value and easily falls into the range of fetal beats. However, due to the quality measurements done before accepting the template to be chosen, this peak will be discarded and the function to search for a new acceptable peak will be called again.

Different approaches to improve this problem could be taken. A way to solve this scenario could be to only give a QRS score if the amplitude is bigger than a certain threshold specified. Furthermore, the score of the amplitude could be multiplied with the score of the QRS width which gives the score of the amplitude a numerical value instead of binary.

Another problem that can be observed by looking at Figure 5.1 and the sub-scores in Table 5.1 and Table 5.2 is that in low amplitude recordings the P-wave scores can be misleading and maybe should not be used since the signal is too low and may not be applicable in these cases. However, due to the rejection mechanism the template is not valid.

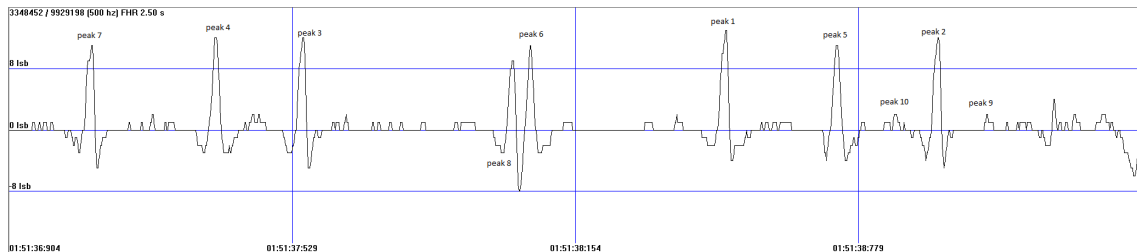


**Figure 5.1:** Wrong peak is chosen with low score amplitude

	Peak 1	Peak 2	Peak 3	Peak 4	Peak 5
Amplitude	13	12	12	12	11
Score amplitude	1	1	1	1	1
Score position	0.7	1	0.3	0.3	0.8
Score QRS width	1	1	1	1	1
Score shape	1	1	1	1	1
Score p shape	0	0	1	0	0
Total score	2.7	3	3.3	2.3	2.8

**Table 5.1:** Scores of Figure 5.1 part 1

	Peak 6	Peak 7	Peak 8	Peak 9
Amplitude	11	11	3	2
Score amplitude	1	1	1	1
Score position	0.3	0.3	0.3	1
Score QRS width	1	1	0.9	1
Score shape	1	1	1	1
Score p shape	0	0	1	1
Total score	2.3	2.3	3.2	4

**Table 5.2:** Scores of Figure 5.1 part 2

On the other hand, it is useful to not discriminate low amplitude peaks since it can also provide some benefits. For example, small peaks that would have been discarded in the original algorithm are now correctly chosen, as it can be seen in Figure 5.2 where peak 2 is the one picked correctly. The sub-scores can be seen in Table 5.3.

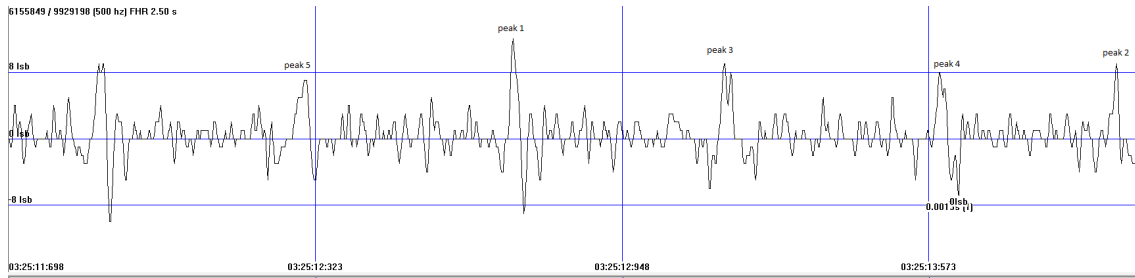


**Figure 5.2:** Good peak is chosen with low score amplitude

	Peak 1	Peak 2	Peak 3	Peak 4	Peak 5
Amplitude	12	9	9	8	7
Score amplitude	1	1	1	1	1
Score position	0.3	1	0.6	0.8	0.3
Score QRS width	1	1	1	1	0.6
Score shape	1	1	1	1	1
Score p shape	1	1	1	0	0
Total score	3.3	4	3.6	3.8	2.9

**Table 5.3:** Scores of Figure 5.2

As a reminder of how the final score is calculated, it was specified in Equation 3.4. Due to that the weight and how the combination of the sub-scores is an optimization problem which is not straightforward to solve. There are possible combinations of the sub-scores that could give better results. Unfortunately, these were not explored at its fullest since this project has limitation and tests that take high amount of time were already performed.

## 5.2 First approach regarding the width of the QRS complex

Regarding the first approach measuring the QRS complex, one problem is that the signal can be inverted. This means that not all negative peaks are S-peaks as it was supposed when implementing the QRS duration procedure which was that all negative peaks were S and all positives were R.

Another problem is that the signal can be noisy and the algorithm is not robust against noise. This can make it difficult to find local maxima and minima when searching for the beginning of Q and the end of S.

Another challenge encountered during the elaboration of this algorithm was that it is easy to have an overfitted model to a specific dataset. For example, the files used for the development could have a specific ECG configuration and these could change even in the same file while the baby is moving during labour. For that reason, a more general approach than the first approach is needed.

### 5.3 Second approach regarding the width of the QRS complex

In the case of the second approach without rejection, the reason 0281 is believed to be worsened is that the rejection mechanism is beneficial in the case of the QRS width and should be something to look into and be improved. The problem that is appearing is that the small peaks are getting a good score regarding the QRS. However, this is something that can be improved by modifying the score of the amplitude as it was discussed in section 5.1. On the other hand, it also shows that the rejection mechanism can be limiting in some cases like 1374. Balancing these two aspects is a trade-off and we still should have in mind to not lose the quality of the HR coverage.

Several examples are shown to understand how the scoring works in some specific cases when it is being beneficial and where it is detrimental and could be improved.

For example, in Figure 5.3, and broken down scores can be seen in Table 5.4, peak 1 is chosen having a total score of 4. However, peak 6 also has a score of 4 because the amplitude score is a binary value and the QRS score could depend on it with a numerical value as an improvement. Because there is a tie, the latest peak (peak 1) is correctly chosen.

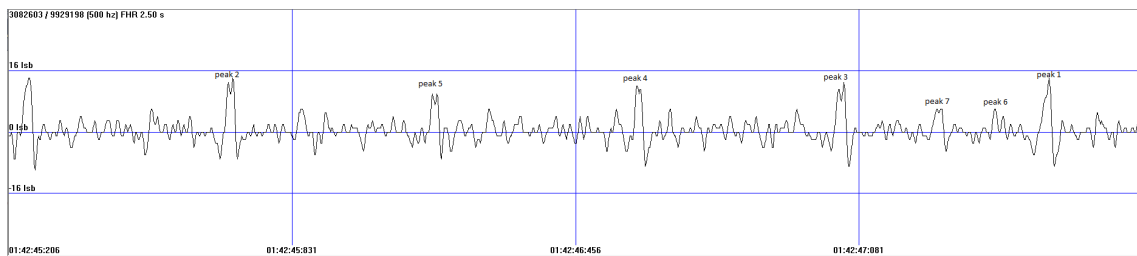


**Figure 5.3:** Good result example with peaks and measurements

	Peak 1	Peak 2	Peak 3	Peak 4	Peak 5	Peak 6	Peak 7
Amplitude	14	14	13	12	10	6	6
Score amplitude	1	1	1	1	1	1	1
Score position	1	0.3	0.7	0.3	0.3	0.8	1
Score QRS width	1	1	0.9	1	1	1	1
Score shape	1	1	1	1	1	1	1
Score p shape	1	1	1	1	1	1	1
Total score	4	3.3	3.6	3.3	3.3	4	3.8

**Table 5.4:** Scores of Figure 5.3

Another example is shown in Figure 5.4 with the scores in Table 5.5. As it can be seen, the maximum score is peak number 2 which is the one chosen even though peak 1 has a higher amplitude which means it is an example of a good outcome.

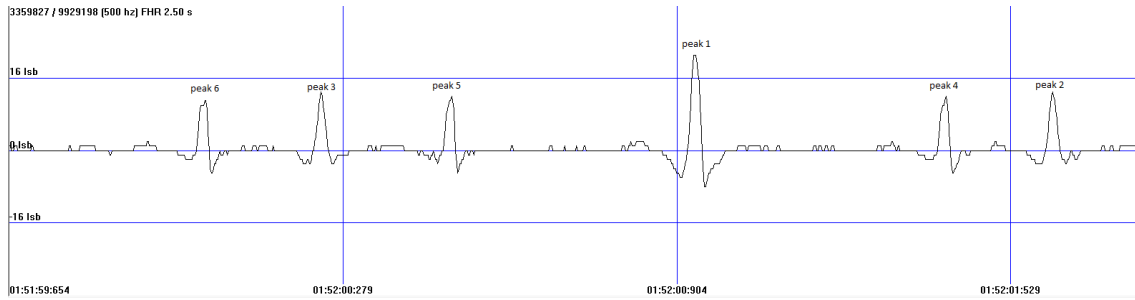


**Figure 5.4:** Good result example with peaks and measurements

	Peak 1	Peak 2	Peak 3	Peak 4	Peak 5	Peak 6
Amplitude	21	13	13	12	12	11
Score amplitude	1	1	1	1	1	1
Score position	0.3	1	0.3	0.8	0.3	0.3
Score QRS width	1	1	1	1	1	1
Score shape	1	1	1	1	1	1
Score p shape	0	1	0	0	0	0
Total score	2.3	4	2.3	2.8	2.3	2.3

**Table 5.5:** Scores of Figure 5.4

One interesting example to study can be seen in Figure 5.5 with its respective peak scores in Table 5.6. Peak 1 is correctly chosen having the maximum score possible. Visually, it can be identified that peak 5 is a maternal peak since the peak is wider than the other peaks. Because of that, the QRS width of peak 5 is 0.9 since it is overlapping in the maternal and fetal range. Also, peaks 6 and 7 are too wide and get a low score regarding the QRS. In this specific case that the amplitudes are between 14 and 35 lsb, the P-wave may be a more reliable and a good score to use.

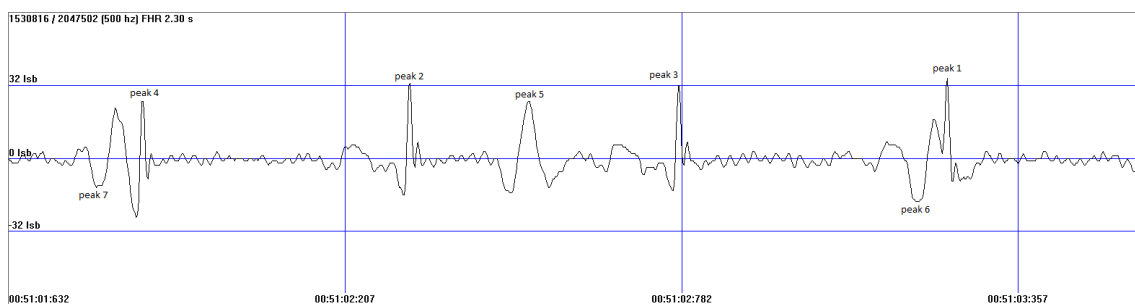


**Figure 5.5:** Good result example with peaks and measurements

Another example where it can be observed that the fetal and maternal peaks are being scored differently are in Figure 5.6 with its score in Table 5.7. Also, it can be observed how the later the peak is the higher it is scored as explained previously.

## 5. Discussion

	Peak 1	Peak 2	Peak 3	Peak 4	Peak 5	Peak 6	Peak 7
Amplitude	35	33	32	26	25	19	13
Score amplitude	1	1	1	1	1	1	1
Score position	1	0.3	0.6	0.3	0.3	0.8	0.3
Score QRS width	1	1	1	1	0.9	0.6	0.6
Score shape	1	1	1	1	1	1	1
Score p shape	1	1	1	1	0	1	1
Total score	4	3.3	3.6	3.3	2.2	3.4	2.9

**Table 5.6:** Scores of Figure 5.5

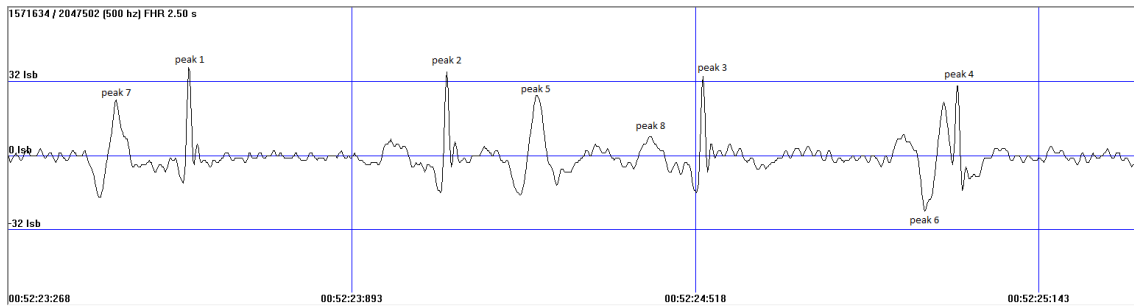


**Figure 5.6:** Good result example with peaks and measurements

	Peak 1	Peak 2	Peak 3	Peak 4	Peak 5
Amplitude	38	36	34	30	26
Score amplitude	1	1	1	1	1
Score position	0.3	0.3	0.6	1	0.3
Score QRS width	1	1	1	1	0.9
Score shape	1	1	1	1	1
Score p shape	1	1	1	1	1
Total score	3.3	3.3	3.6	4	3.2

**Table 5.7:** Scores of Figure 5.6

A bad result can be seen in Figure 5.7 and the respective scores in Table 5.8. This example is useful to know for aiming to improve the algorithm. However, even if it is chosen bad, in the case of the rejection algorithm this peak will be discarded because it is not twice as large as the second highest peak around. Therefore, we see an improvement when the rejection measurements are applied. The reason why there is improvements with rejection mechanism is due to it is ensuring quality in the template chosen. Also, we can observe that giving too much value to the P-wave score could have a disadvantage because even after peak 12, the next peak would have been peak 2 because the P-wave score is 1 in there and 0 in peak 1, even though the peak 1 is later.

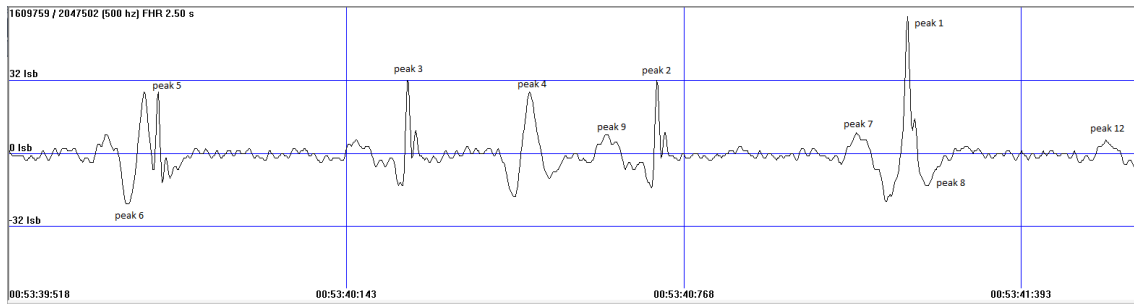


**Figure 5.7:** Bad result example with peaks and measurements

	Peak 1	Peak 2	Peak 4	Peak 6	Peak 7	Peak 12
Amplitude	60	32	27	22	9	4
Score amplitude	1	1	1	1	1	1
Score position	0.8	0.6	0.3	0.3	0.8	1
Score QRS width	1	1	0.9	0.9	0.6	1
Score shape	1	1	1	1	1	1
Score p shape	0	1	0	1	1	1
Total score	2.8	3.6	2.2	3.2	3.4	4

**Table 5.8:** Scores of Figure 5.7

In this example, Figure 5.8 and scores in Table 5.9, even though the maternal peaks have higher amplitude, the algorithm is capable to pick the fetal beat due to the amplitude of the width. This is an excellent example that the second approach used for the QRS width has good outcomes and can be beneficial.

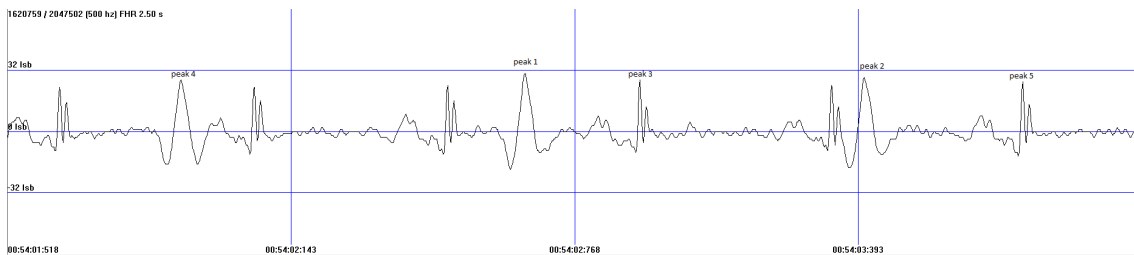


**Figure 5.8:** Good result example with peaks and measurements

	Peak 1	Peak 2	Peak 3	Peak 4	Peak 5
Amplitude	30	28	27	27	26
Score amplitude	1	1	1	1	1
Score position	0.3	0.8	0.6	0.3	1
Score QRS width	1	0.9	1	0.9	1
Score shape	1	1	1	1	1
Score p shape	1	1	1	0	1
Total score	3.3	3.7	3.6	2.2	4

**Table 5.9:** Scores of Figure 5.8

## 5. Discussion

In the case of Figure 5.9 and Table 5.10, even if the maternal peak (peak 3) is the latest, the fetal peak (peak 5) is the one chosen and being correct which would not have happened in the original algorithm. The peak is chosen correctly since it is given priority for being in the width of the fetal range and having a measurable P-wave. However, peak 12 which is actually a P-wave is almost chosen but thanks to that in case of having a tie in score the latest peak is the one chosen peak 5 is taken which in this case is beneficial and the correct peak.

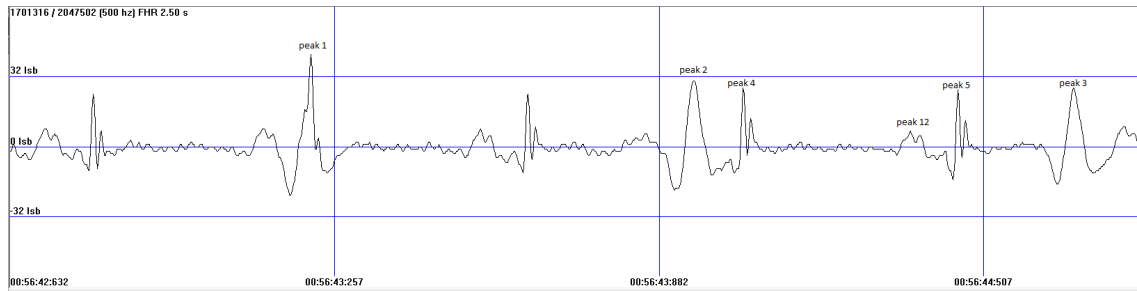


**Figure 5.9:** Good result example with peaks and measurements

	Peak 1	Peak 2	Peak 3	Peak 4	Peak 5	Peak 12
Amplitude	42	30	27	27	26	7
Score amplitude	1	1	1	1	1	1
Score position	0.3	0.6	1	0.6	0.8	0.8
Score QRS width	1	0.9	0.9	1	1	1
Score shape	1	1	1	1	1	1
Score p shape	0	1	0	1	1	1
Total score	2.3	3.5	2.9	3.6	3.8	3.8

**Table 5.10:** Scores of Figure 5.9

As it can be seen in Figure 5.10 with scores in Table 5.11, the correct peak which is number 5 is chosen even though peak 6 is in the beneficial position range at the end of the window. The decisive difference is that peak 5 is in the fetal width range and also has a measurable P-wave.

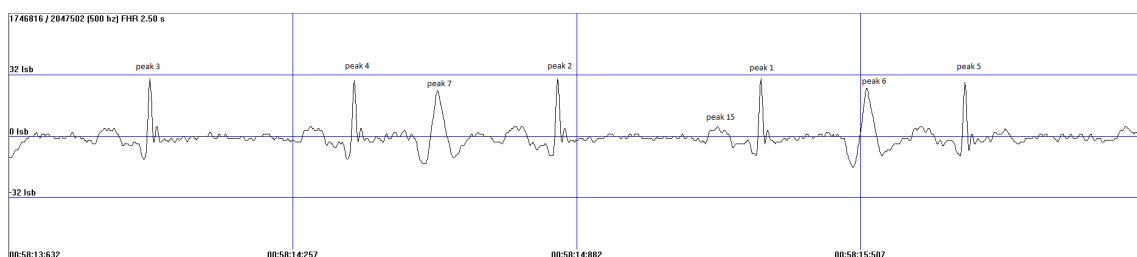


**Figure 5.10:** Good result example with peaks and measurements

	Peak 1	Peak 2	Peak 3	Peak 4	Peak 5	Peak 6
Amplitude	30	30	30	29	28	25
Score amplitude	1	1	1	1	1	1
Score position	0.8	0.3	0.3	0.3	1	1
Score QRS width	1	0.9	0.9	1	1	0.9
Score shape	1	1	1	1	1	1
Score p shape	0	0	0	0	1	0
Total score	2.8	2.3	2.3	2.3	4	2.9

**Table 5.11:** Scores of Figure 5.10

In summary, after looking at the results and the examples, it was concluded that the second approach with rejection mechanism is the approach that has improved the average coverage and also decreased the values below 100 HR while not losing too many HR amount on the process. In addition, it has improved the variability (meaning less amount of maternal beats) while preserving quality coverage.

Furthermore, since the second approach is more general than the first, it was deduced that it will work better in diverse ECG configurations and not only in the case of an ideal ECG and that is why it was the approach chosen to move forward. Also, it was decided to use it with rejection mechanisms since the results are better and ensure that quality of the template is good enough for the other parameters used and also solves some of the problems with the scoring not working in all cases.

## 5.4 Neoventa database

As seen in section 4.2, the new algorithm approach has slightly improved the coverage. Since the challenge that this thesis aimed to solve is small statistically speaking, it is normal that the coverage has not improved significantly. However, it is important to note that the coverage has not gotten worse.

Based on the results of the Neoventa database it would be possible to identify new files where the maternal beat is presented as the fetal beat and evaluate the algorithm based on those files.

## 5.5 Future work

Unfortunately, because of the time limit of this thesis, only a certain amount of iterations could be done. However, some ideas to improve the algorithm even further were found which could be investigated in the future.

One way in which the algorithm could be changed is by decreasing the amount of peaks. At the beginning it was thought that the amount of peaks would not affect the output results. This could be true if the score was working as intended in all the cases. However, there are some edge cases that have to be fixed to not affect

the template chosen. Also, the amount of peaks could affect the efficiency of the algorithm which was not studied during the development of this project.

Another part that could be explored in the future is to improve the rejection mechanisms and adapting them into not limiting the score of the peaks chosen but having a balance to still keep quality in the template for the other parameters used in the program.

In addition, improving the amplitude score and having some balance between giving priority to the biggest peaks and not discriminating low amplitude beats would be interesting to explore.

Another area to research that could be beneficial for the algorithm is how to optimize the sub-scores to maximize the correct peak chosen. There are different parts that could be explored for example how to combine them with addition, multiplication, division or other operations. Furthermore, weighting and scaling the parameters and choosing an appropriate value for this which could be done using a constant but also in a linear, logarithmic or exponential way.

Also, it would be helpful to have statistical data of the maternal beat at 50% of the peak to study in more detail where the distributions are overlapping.

Furthermore, it would be interesting to explore the final results with the Neoventa database at individual files level to identify potential problems that have not yet been discovered.

In addition, performing a new evaluation of the algorithm in only known files where the maternal beat is presented as fetal beat could be useful to visualize.

# 6

## Conclusion

The purpose of this thesis was to develop an algorithm that can differentiate between maternal and fetal beats and act upon that. This was accomplished with the new design for a template to be chosen.

The major findings concluded from the literature study were that there is no presence of P-wave with the FSE configuration since the maternal signal is too weak to reach the thigh. Another finding was that the QRS width is shorter in fetuses than in adults and this property was exploited to differentiate between maternal and fetal beats.

Two approaches were conducted to solve the differentiation between maternal and fetal beats. One approach was based on the literature study output which did not anticipate about diverse ECG configurations and other problems related with this. On the other hand, the other approach was a combination between the literature study and statistical values concluded from the Neoventa database. This solved some of the problems encountered in the first approach but made other problems appear. It was also discovered that the rejection mechanism to ensure the quality of the signal could limit the template chosen since it might be rejected later but was also beneficial in some scenarios.

The results made in the Neoventa database are categorized by quarters and machines used. It can be seen that the algorithm developed has improved the coverage slightly (around 0.07%) but could be improved more by exploring different options such as implementing a new amplitude score, optimizing the sub-scores and acquiring useful statistical data regarding the maternal beats among others.



# Bibliography

- [1] K. G. Rosén and A. Mårtendal, *The Green book of Neoventa part I – The physiology of fetal surveillance*. 2014.
- [2] Neoventa Medical. “About us,” [Online]. Available: [https://www.neoventa.com/about\\_us/](https://www.neoventa.com/about_us/) (visited on 01/25/2021).
- [3] C. b. Agateller, *Schematic diagram of normal sinus rhythm for a human heart as seen on ECG (with english labels)*. Jan. 13, 2007. [Online]. Available: <https://commons.wikimedia.org/wiki/File:SinusRhythmLabels.svg> (visited on 01/25/2021).
- [4] A.-K. Welin, H. Norén, A. Odeback, M. Andersson, G. Andersson, and K. G. Rosén, “STAN, a clinical audit: The outcome of 2 years of regular use in the city of varberg, sweden,” *Acta Obstetricia et Gynecologica Scandinavica*, vol. 86, no. 7, pp. 827–832, 2007, ISSN: 1600-0412. DOI: <https://doi.org/10.1080/00016340701416903>. [Online]. Available: <https://obgyn.pericles-rod.literatumonline.com/doi/abs/10.1080/00016340701416903> (visited on 01/26/2021).
- [5] G. Straface, G. Scambia, and V. Zanardo, “Does ST analysis of fetal ECG reduce cesarean section rate for fetal distress?” *J Matern Fetal Neonatal Med*, p. 5, Sep. 2, 2016.
- [6] B. Aehlert, *ECGs made easy*, Sixth edition. Phoenix, Arizona: Southwest EMS Education, Inc, 2018, 326 pp., ISBN: 978-0-323-40130-2.
- [7] B. Picazo-Angelin, J. I. Zabala-Argüelles, R. H. Anderson, and D. Sánchez-Quintana, “Anatomy of the normal fetal heart: The basis for understanding fetal echocardiography,” *Annals of Pediatric Cardiology*, vol. 11, no. 2, pp. 164–173, 2018, ISSN: 0974-2069. DOI: 10.4103/apc.APC\_152\_17. [Online]. Available: <https://www.ncbi.nlm.nih.gov/pmc/articles/PMC5963230/> (visited on 05/22/2021).
- [8] “File:diagram of the human heart (cropped).svg - wikimedia commons,” [Online]. Available: [https://commons.wikimedia.org/wiki/File:Diagram\\_of\\_the\\_human\\_heart\\_\(cropped\).svg](https://commons.wikimedia.org/wiki/File:Diagram_of_the_human_heart_(cropped).svg) (visited on 04/13/2021).
- [9] G. J. Tortora and B. Derrickson, *Introduction to the human body: the essentials of anatomy and physiology*, Tenth edition. Hoboken, NJ: John Wiley & Sons, 2015, 1 p., ISBN: 978-1-118-58318-0.
- [10] O. College, *Illustration from anatomy & physiology, connexions*. [Online]. Available: [https://commons.wikimedia.org/wiki/File:2023\\_ECG\\_Tracing\\_with\\_Heart\\_ContractionN.jpg](https://commons.wikimedia.org/wiki/File:2023_ECG_Tracing_with_Heart_ContractionN.jpg) (visited on 04/28/2021).
- [11] C. Gleason and S. Juul, *Avery’s Diseases of the Newborn*. Elsevier, 2005, ISBN: 978-0-7216-9347-7. DOI: 10.1016/B978-0-7216-9347-7.X5001-X.

- [Online]. Available: <https://linkinghub.elsevier.com/retrieve/pii/S1521693477X5001X> (visited on 04/28/2021).
- [12] I. Amer-Wahlin and A. Kwee, “Combined cardiotocographic and ST event analysis: A review,” *Best Practice & Research Clinical Obstetrics & Gynaecology*, Intrapartum Fetal Surveillance, vol. 30, pp. 48–61, Jan. 1, 2016, ISSN: 1521-6934. DOI: 10.1016/j.bpobgyn.2015.05.007. [Online]. Available: <http://www.sciencedirect.com/science/article/pii/S1521693415001078> (visited on 01/20/2021).
- [13] B. H. A. Wattar, E. Honess, S. Bunnewell, N. J. Welton, S. Quenby, K. S. Khan, J. Zamora, and S. Thangaratnam, “Effectiveness of intrapartum fetal surveillance to improve maternal and neonatal outcomes: A systematic review and network meta-analysis,” *CMAJ*, vol. 193, no. 14, E468–E477, Apr. 6, 2021, Publisher: CMAJ Section: Research, ISSN: 0820-3946, 1488-2329. DOI: 10.1503/cmaj.202538. [Online]. Available: <http://www.cmaj.ca/content/193/14/E468> (visited on 04/28/2021).
- [14] Neoventa Medical. “Mission & vision,” [Online]. Available: [https://www.neoventa.com/about\\_us/mission-vision/](https://www.neoventa.com/about_us/mission-vision/) (visited on 04/28/2021).
- [15] H. Norén and A. Carlsson, “Reduced prevalence of metabolic acidosis at birth: An analysis of established STAN usage in the total population of deliveries in a swedish district hospital,” *American Journal of Obstetrics and Gynecology*, vol. 202, no. 6, 546.e1–7, Jun. 2010, ISSN: 1097-6868. DOI: 10.1016/j.ajog.2009.11.033.
- [16] E. Chandrachan, “Foetal electrocardiograph (ST-analyser or STAN) for intrapartum foetal heart rate monitoring: A friend or a foe?” *The Journal of Maternal-Fetal & Neonatal Medicine*, vol. 31, no. 1, pp. 123–127, Jan. 2, 2018, ISSN: 1476-7058, 1476-4954. DOI: 10.1080/14767058.2016.1276559. [Online]. Available: <https://www.tandfonline.com/doi/full/10.1080/14767058.2016.1276559> (visited on 01/26/2021).
- [17] K. G. Rosén, I. Amer-Wåhlin, R. Luzietti, and H. Norén, “Fetal ECG waveform analysis,” *Best Practice & Research Clinical Obstetrics & Gynaecology*, Fetal Surveillance, vol. 18, no. 3, pp. 485–514, Jun. 1, 2004, ISSN: 1521-6934. DOI: 10.1016/j.bpobgyn.2004.02.008. [Online]. Available: <http://www.sciencedirect.com/science/article/pii/S1521693404000343> (visited on 01/26/2021).
- [18] C. Liu, P. Li, C. Di Maria, L. Zhao, H. Zhang, and Z. Chen, “A multi-step method with signal quality assessment and fine-tuning procedure to locate maternal and fetal QRS complexes from abdominal ECG recordings,” *Physiological Measurement*, vol. 35, no. 8, pp. 1665–1683, Aug. 1, 2014, ISSN: 0967-3334, 1361-6579. DOI: 10.1088/0967-3334/35/8/1665. [Online]. Available: <https://iopscience.iop.org/article/10.1088/0967-3334/35/8/1665> (visited on 01/26/2021).
- [19] R. Martinek, R. Kahankova, J. Jezewski, R. Jaros, J. Mohylova, M. Fajkus, J. Nedoma, P. Janku, and H. Nazeran, “Comparative effectiveness of ICA and PCA in extraction of fetal ECG from abdominal signals: Toward non-invasive fetal monitoring,” *Frontiers in Physiology*, vol. 9, 2018, Publisher: Frontiers, ISSN: 1664-042X. DOI: 10.3389/fphys.2018.00648. [Online]. Available: <http://www.frontiersin.org>

- [//www.frontiersin.org/articles/10.3389/fphys.2018.00648/full](http://www.frontiersin.org/articles/10.3389/fphys.2018.00648/full) (visited on 01/26/2021).
- [20] F. Yano and S. P. Ninomija, "A detecting method for the fetal QRS complex with a small amplitude," *Journal of Medical Systems*, vol. 10, no. 4, pp. 307–320, Aug. 1986, ISSN: 0148-5598, 1573-689X. DOI: 10.1007/BF00992433. [Online]. Available: <http://link.springer.com/10.1007/BF00992433> (visited on 01/27/2021).
- [21] V. Smith, S. Arunthavanathan, A. Nair, D. Ansermet, F. da Silva Costa, and E. M. Wallace, "A systematic review of cardiac time intervals utilising non-invasive fetal electrocardiogram in normal fetuses," *BMC Pregnancy and Childbirth*, vol. 18, Sep. 12, 2018, ISSN: 1471-2393. DOI: 10.1186/s12884-018-2006-8. [Online]. Available: <https://www.ncbi.nlm.nih.gov/pmc/articles/PMC6134593/> (visited on 01/29/2021).
- [22] Neoventa Medical. "Fetal ECG waveform – helps differentiating maternal from fetal heart rate « neoventa medical," [Online]. Available: <https://www.neoventa.com/2012/10/new-publication-fetal-ecg-waveform-helps-differentiating-maternal-from-fetal-heart-rate/> (visited on 01/29/2021).
- [23] R. Nurani, E. Chandrachan, V. Lowe, A. Ugwumadu, and S. Arulkumaran, "Misidentification of maternal heart rate as fetal on cardiotocography during the second stage of labor: The role of the fetal electrocardiograph: Erroneous recording of maternal heart rate," *Acta Obstetrica et Gynecologica Scandinavica*, vol. 91, no. 12, pp. 1428–1432, Dec. 2012, ISSN: 00016349. DOI: 10.1111/j.1600-0412.2012.01511.x. [Online]. Available: <http://doi.wiley.com/10.1111/j.1600-0412.2012.01511.x> (visited on 01/29/2021).
- [24] D. J. Sherman, E. Frenkel, Y. Kurzweil, A. Padua, S. Arieli, and M. Bahar, "Characteristics of maternal heart rate patterns during labor and delivery," vol. 99, no. 4, p. 6, 2002.
- [25] Ahmad Jaafar and Dragos Predescu, *Pediatric ECG survival guide*, 2018.
- [26] S. M, "Electrocardiographic q RS axis, q wave and t-wave changes in 2 nd and 3 rd trimester of normal pregnancy," *JOURNAL OF CLINICAL AND DIAGNOSTIC RESEARCH*, 2014, ISSN: 2249782X. DOI: 10.7860/JCDR/2014/10037.4911. [Online]. Available: [http://www.jcdr.net/article\\_fulltext.asp?issn=0973-709x&year=2014&volume=8&issue=9&page=BC17&issn=0973-709x&id=4911](http://www.jcdr.net/article_fulltext.asp?issn=0973-709x&year=2014&volume=8&issue=9&page=BC17&issn=0973-709x&id=4911) (visited on 01/26/2021).
- [27] M. Malik, Ed., *Sex and cardiac electrophysiology: differences in cardiac electrical disorders between men and women*, 1st ed., Waltham: Elsevier, 2020, ISBN: 978-0-12-817728-0.
- [28] K. Hnatkova, P. Smetana, O. Toman, G. Schmidt, and M. Malik, "Sex and race differences in QRS duration," p. 8, May 5, 2016.
- [29] S. Pildner von Steinburg, A.-L. Boulesteix, C. Lederer, S. Grunow, S. Schiermeier, W. Hatzmann, K.-T. M. Schneider, and M. Daumer, "What is the "normal" fetal heart rate?" *PeerJ*, vol. 1, Jun. 4, 2013, ISSN: 2167-8359. DOI: 10.7717/peerj.82. [Online]. Available: <https://www.ncbi.nlm.nih.gov/pmc/articles/PMC3678114/> (visited on 04/27/2021).
- [30] S. S. Bhatia, W. H. Burgess, and J. R. Skinner, "Fetal tachycardia in the delivery room: Fetal distress, supraventricular tachycardia, or both?" *AJP*

*Reports*, vol. 10, no. 4, e380–e385, Oct. 2020, ISSN: 2157-6998. DOI: 10.1055/s-0040-1718900. [Online]. Available: <https://www.ncbi.nlm.nih.gov/pmc/articles/PMC7669433/> (visited on 04/27/2021).

# A

## Appendix 1

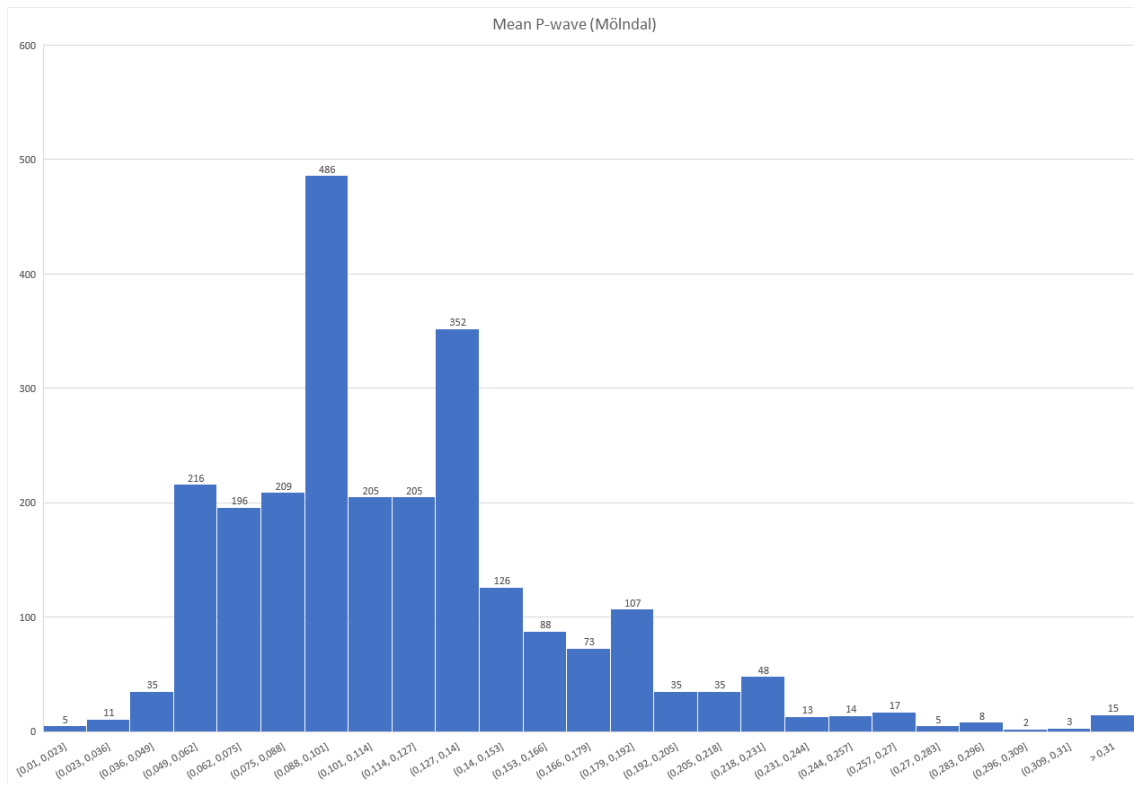


**Figure A.1:** Histogram of the mean value of the P-wave (round 2 decimals)

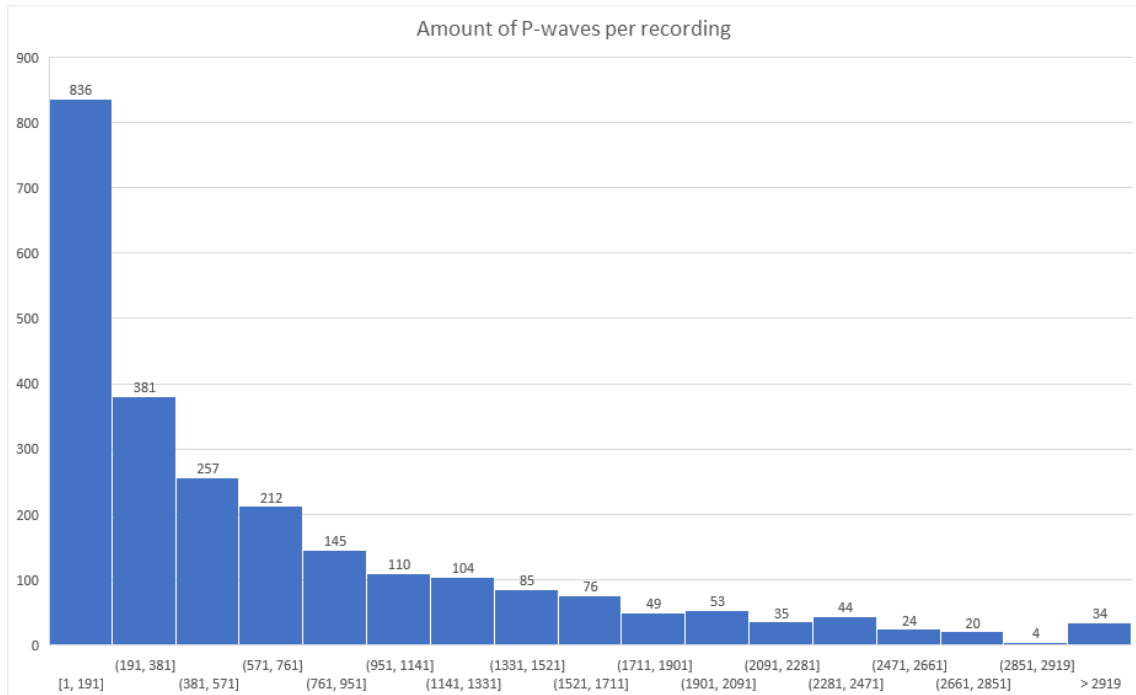


Figure A.2: Histogram of the number of P-waves

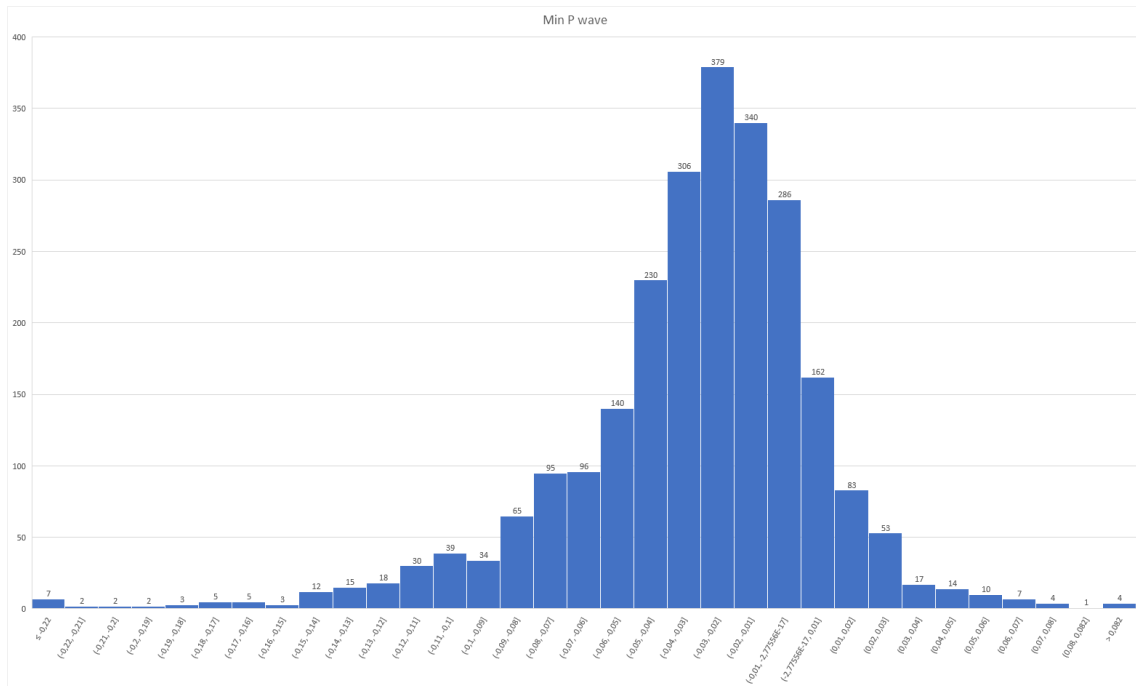


Figure A.3: Histogram of minimum P-wave value

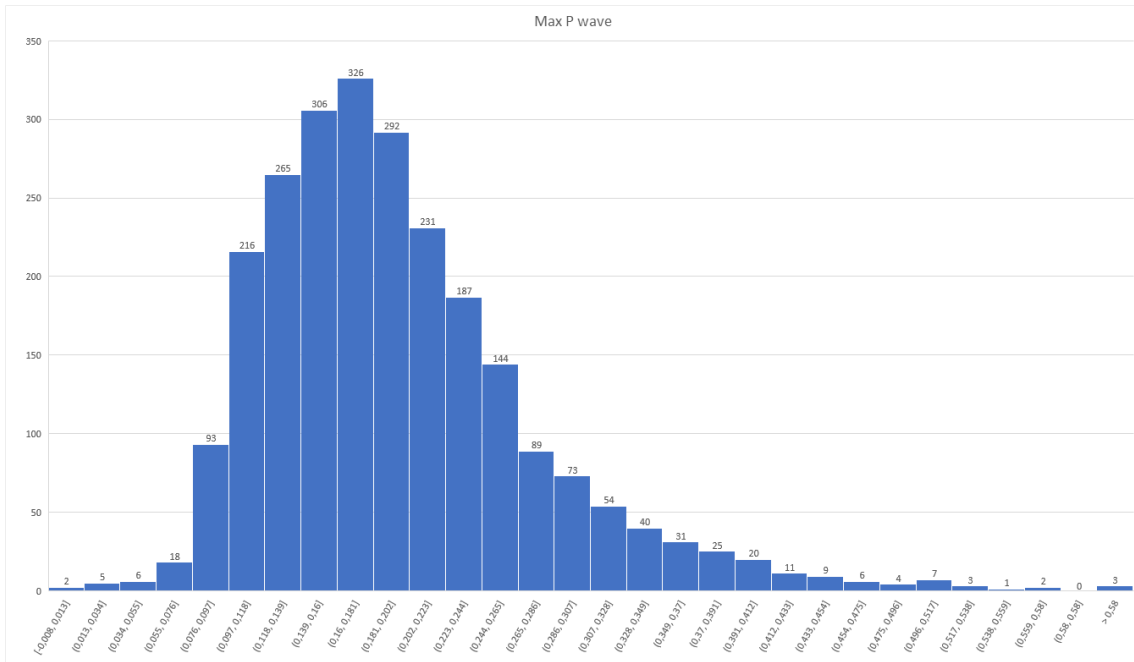


Figure A.4: Histogram of maximum P-wave value

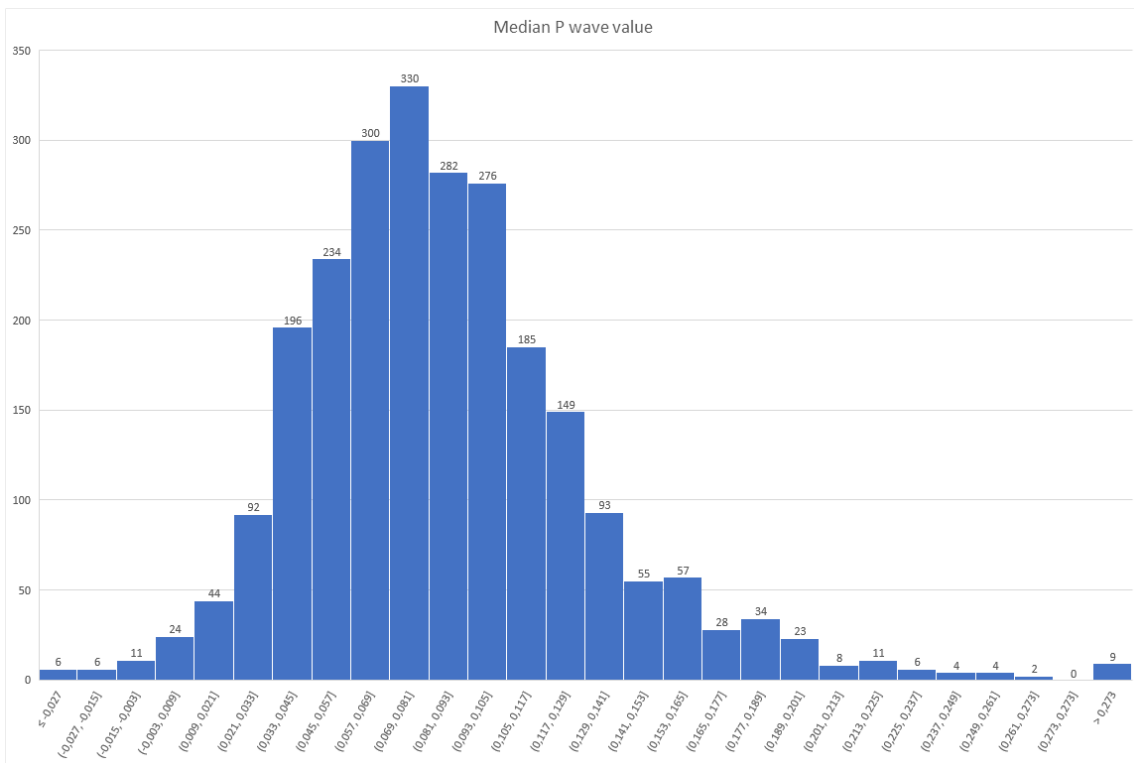


Figure A.5: Histogram of median P-wave value



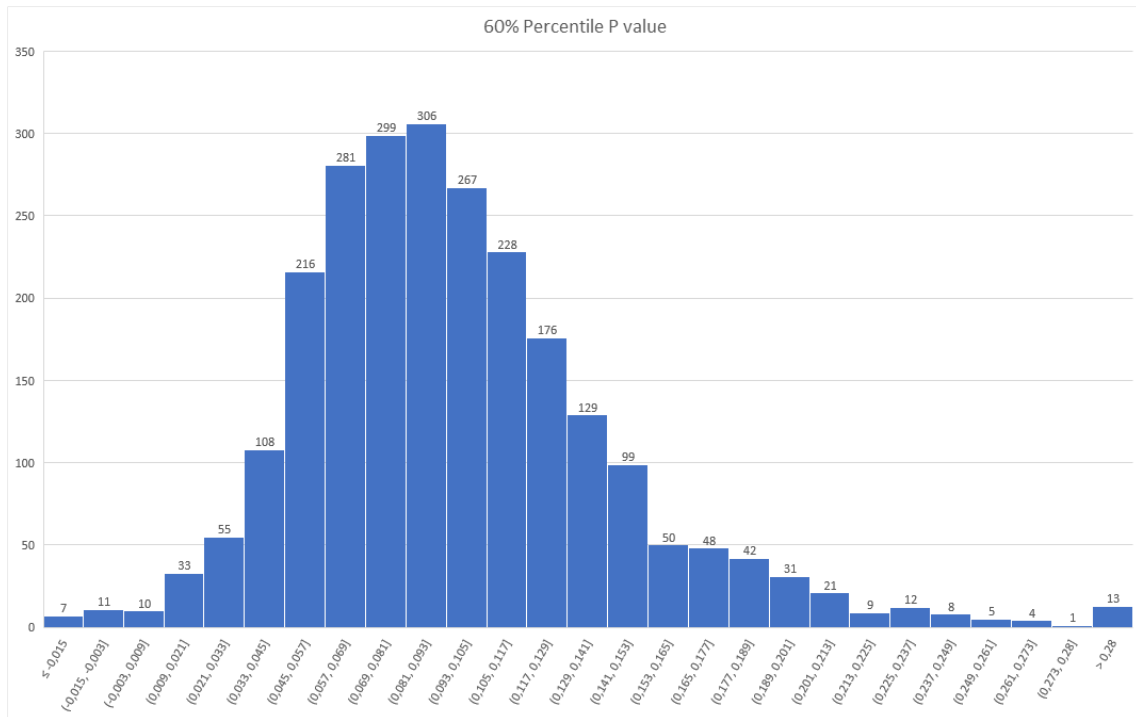


Figure A.8: Histogram of the 60% percentile of the P-wave value

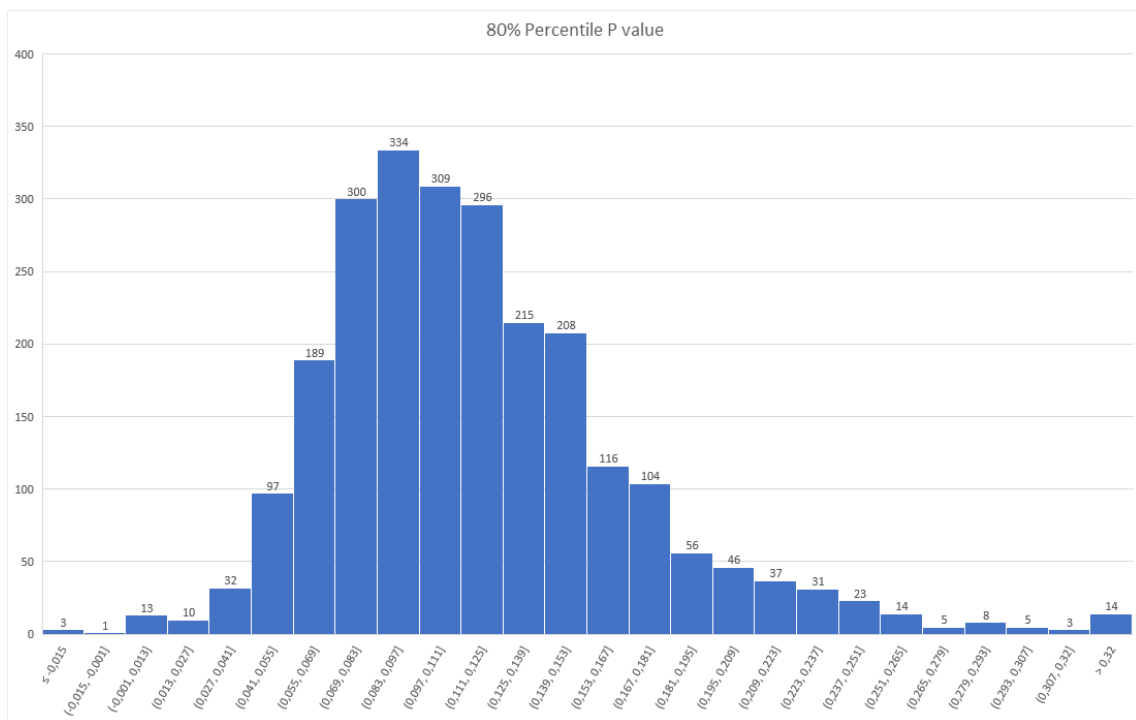


Figure A.9: Histogram of the 80% percentile of the P-wave value

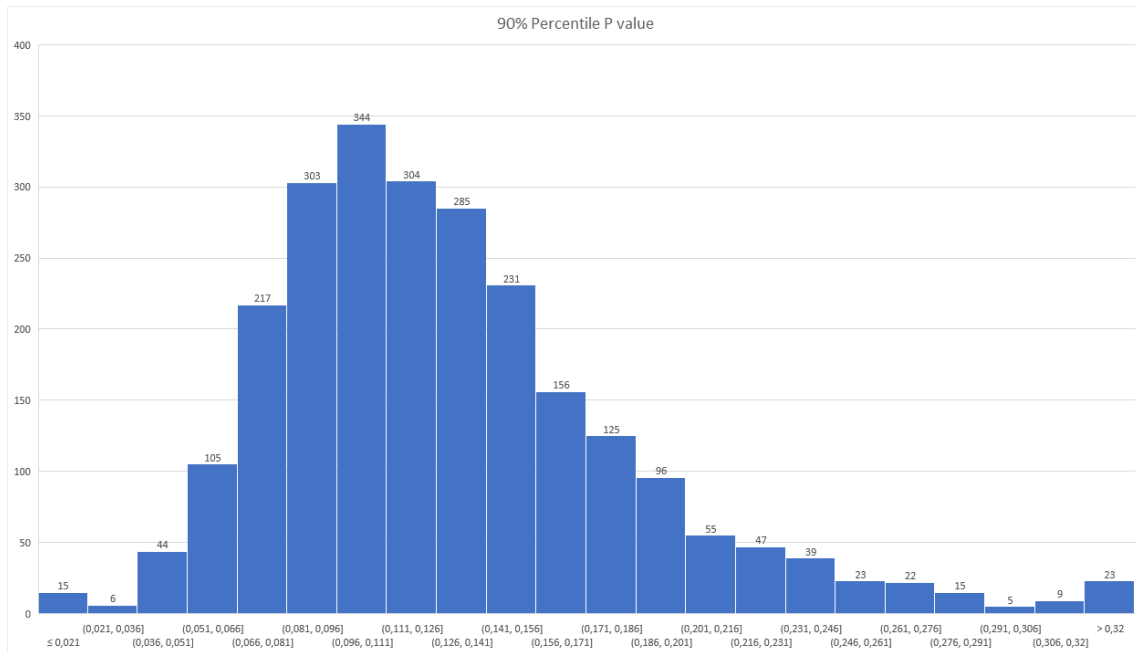


Figure A.10: Histogram of the 90% percentile of the P-wave value

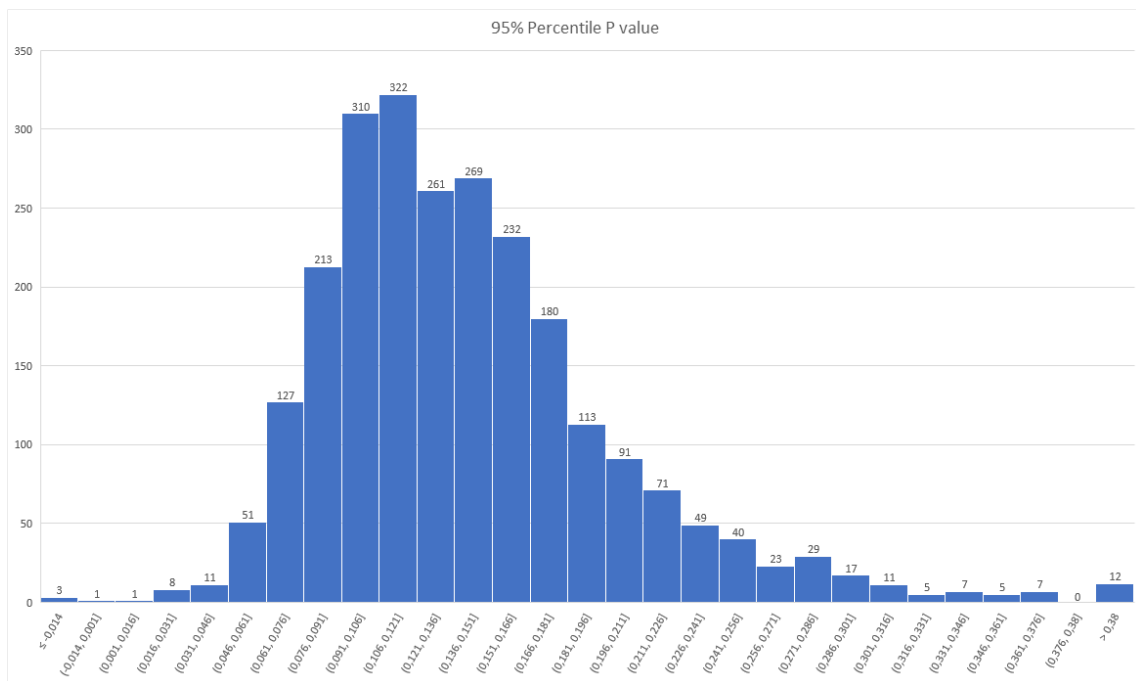


Figure A.11: Histogram of the 95% percentile of the P-wave value

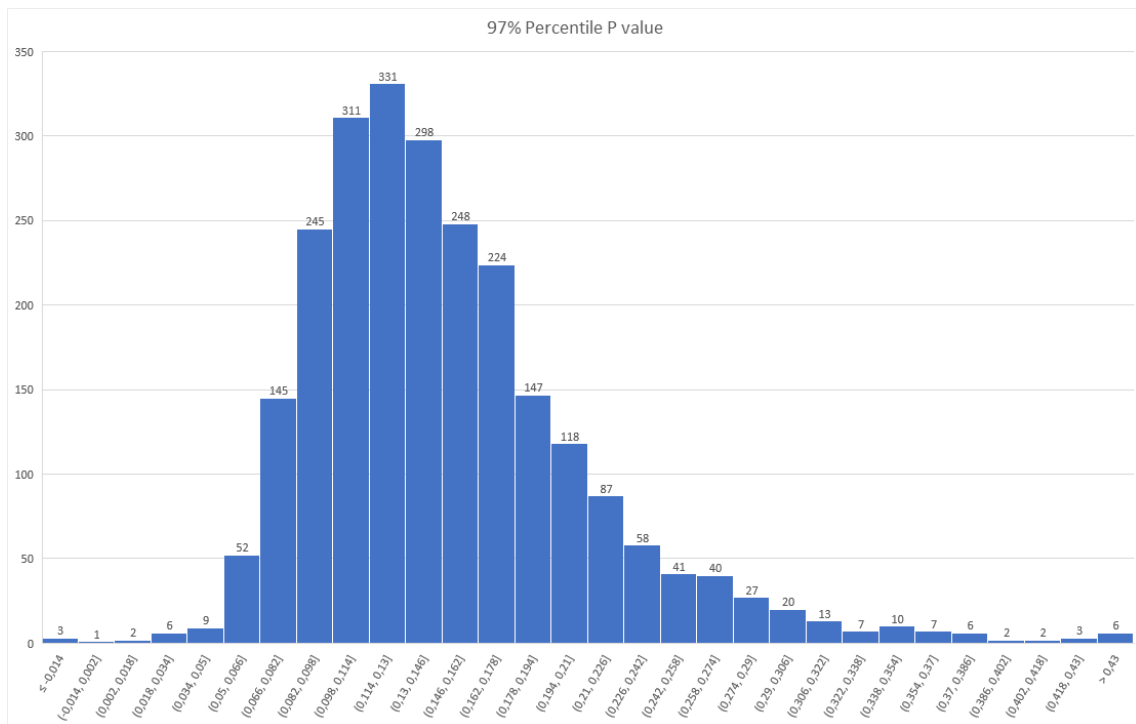


Figure A.12: Histogram of the 97% percentile of the P-wave value

DEPARTMENT OF ELECTRICAL ENGINEERING  
CHALMERS UNIVERSITY OF TECHNOLOGY  
Gothenburg, Sweden  
[www.chalmers.se](http://www.chalmers.se)



**CHALMERS**  
UNIVERSITY OF TECHNOLOGY